CO_2 exchange between air and water in an Arctic Alaskan and midlatitude Swiss lake: Importance of convective mixing

Werner Eugster,[1] George Kling,[2] Tobias Jonas,[3] Joseph P. McFadden,[4] Alfred Wüest,[3] Sally MacIntyre,[5] and F. Stuart Chapin III[6]

Received 14 June 2002; revised 9 January 2003; accepted 11 March 2003; published 24 June 2003.

[1] CO_2 exchange between lake water and the atmosphere was investigated at Toolik Lake (Alaska) and Soppensee (Switzerland) employing the eddy covariance (EC) method. The results obtained from three field campaigns at the two sites indicate the importance of convection in the lake in driving gas flux across the water-air interface. Measurements were performed during short (1–3 day) periods with observed diurnal changes between stratified and convective conditions in the lakes. Over Toolik Lake the EC net CO_2 efflux was 114 ± 33 mg C m^{-2} d^{-1}, which compares well with the 131 ± 2 mg C m^{-2} d^{-1} estimated by a boundary layer model (BLM) and the 153 ± 3 mg C m^{-2} d^{-1} obtained with a surface renewal model (SRM). Floating chamber measurements, however, indicated a net efflux of 365 ± 61 mg C m^{-2} d^{-1}, which is more than double the EC fluxes measured at the corresponding times (150 ± 78 mg C m^{-2} d^{-1}). The differences between continous (EC, SRM, and BLM) and episodic (chamber) flux determination indicate that the chamber measurements might be biased depending on the chosen sampling interval. Significantly smaller fluxes ($p < 0.06$) were found during stratified periods (51 ± 42 mg C m^{-2} d^{-1}) than were found during convective periods (150 ± 45 mg C m^{-2} d^{-1}) by the EC method, but not by the BLM. However, the congruence between average values obtained by the models and EC supports the use of both methods, but EC measurements and the SRM provide more insight into the physical-biological processes affecting gas flux. Over Soppensee, the daily net efflux from the lake was 289 ± 153 mg C m^{-2} d^{-1} during the measuring period. Flux differences were significant ($p < 0.002$) between stratified periods (240 ± 82 mg C m^{-2} d^{-1}) and periods with penetrative convection (1117 ± 236 mg C m^{-2} d^{-1}) but insignificant if convection in the lake was weak and nonpenetrative. Our data indicate the importance of periods of heat loss and convective mixing to the process of gas exchange across the water surface, and calculations of gas transfer velocity using the surface renewal model support our observations. Future studies should employ the EC method in order to obtain essential data for process-scale investigations. Measurements should be extended to cover the full season from thaw to freeze, thereby integrating data over stratified and convective periods. Thus the statistical confidence in the seasonal budgets of CO_2 and other trace gases that are exchanged across lake surfaces could be increased considerably. *INDEX TERMS:* 0315 Atmospheric Composition and Structure: Biosphere/atmosphere interactions; 3307 Meteorology and Atmospheric Dynamics: Boundary layer processes; 0322 Atmospheric Composition and Structure: Constituent sources and sinks; 1845 Hydrology: Limnology; 1806 Hydrology: Chemistry of fresh water; *KEYWORDS:* carbon dioxide efflux, gas evasion from lakes, CO_2 flux, eddy covariance, turbulent mixing, water-atmosphere interactions

Citation: Eugster, W., G. Kling, T. Jonas, J. P. McFadden, A. Wüest, S. MacIntyre, and F. S. Chapin III, CO_2 exchange between air and water in an Arctic Alaskan and midlatitude Swiss lake: Importance of convective mixing, *J. Geophys. Res.*, *108*(D12), 4362, doi:10.1029/2002JD002653, 2003.

[1]Geographical Institute, University of Bern, Bern, Switzerland.
[2]Department of Ecology and Evolutionary Biology, University of Michigan, Ann Arbor, Michigan, USA.
[3]Swiss Federal Institute for Environmental Science and Technology, Dübendorf, Switzerland.
[4]Department of Ecology, Evolution, and Behavior, University of Minnesota, St. Paul, Minnesota, USA.
[5]Marine Science Institute and Institute for Computational Earth System Science, University of California, Santa Barbara, California, USA.
[6]Institute of Arctic Biology, University of Alaska, Fairbanks, Alaska, USA.

Copyright 2003 by the American Geophysical Union.
0148-0227/03/2002JD002653

1. Introduction

[2] The exchange of gases across the air-water interface is mediated by turbulence from wind shear, convection due to heat loss at the surface, rainfall, and microscale and large-scale wave breaking. All these processes induce turbulence near the air-water interface, and turbulent eddies and their associated vorticity are required for gas fluxes to occur. While turbulence due to wave breaking induces large fluxes in the oceans, similar processes affect gas fluxes in lakes and oceans when wind speeds are between 3 and 8 m s^{-1}. At these wind speeds, both microscale wave breaking, convection in the water body, and wind shear contribute to aquatic turbulence. The few studies in lakes that consider high and moderate wind speeds indicate that energy dissipation rates, which represent the magnitude of turbulence in the surface waters of lakes, are comparable to conditions in oceans [*MacIntyre et al.*, 1999]. Below wind speeds of 3 m s^{-1}, gas flux is independent of wind speed [*Ocampo-Torres et al.*, 1994]. A number of empirical formulations have been derived in order to describe gas flux, of which most are based on wind speed [*MacIntyre et al.*, 1995; *Cole and Caraco*, 1998; *Wanninkhof and McGillis*, 1999]. The contribution due to convection in the water is poorly understood. Convection is likely to be the dominant mechanism causing gas flux at low wind speeds. Energy budget analyses indicate that current parameterizations will likely underestimate gas fluxes by a factor of two in tropical environments, where evaporation is a major component of the surface energy budget [*MacIntyre et al.*, 2001]. The contribution of heat flux has been included in one formulation for gas fluxes [*Soloviev and Schluessel*, 1994, 2001], but this was derived for the oceans and has not been satisfactorily applied to small lakes [*Anderson et al.*, 1999]. Lakes are often topographically sheltered, affording them protection against strong winds [*Schladow et al.*, 2002; *Kocsis et al.*, 1999], which makes the application of oceanographically derived formulations questionable under such conditions [*Schladow et al.*, 2002]. *Cole et al.* [1994] showed that CO_2 flux from small lakes to the atmosphere can be a large component of the carbon budget, and even of the surrounding landscape [*Kling et al.*, 1991, 1992; *Richey et al.*, 2002]. Therefore it is imperative that the processes controlling gas exchange with the atmosphere are well understood and ultimately included in parameterizations of the gas transfer velocity.

[3] Over the past decade, the eddy covariance (EC) method [e.g., *Arya*, 1988; *Lenschow*, 1995] has become established as the preferred approach for direct measurements of fluxes over terrestrial surfaces. Pioneer studies employing the EC technique have also been carried out to investigate trace gas exchange at the ocean surface [e.g., *Jones and Smith*, 1977; *Francey and Garratt*, 1978; *Wesely et al.*, 1982; *Smith and Jones*, 1985, 1986; *Smith et al.*, 1991; *McGillis et al.*, 2001] and across lakes [e.g., *Edwards et al.*, 1994; *Anderson et al.*, 1999]. However, EC measurements over lakes have so far shown significant disagreement with other techniques [see *Anderson et al.*, 1999; *Fairall et al.*, 2000]. Many of the studies of gas fluxes from small water bodies have relied on floating chamber methods, but these methods have been criticized [e.g., *Belanger and Korzun*, 1990; *Stephens*, 1978; *Livingston and Hutchinson*, 1995]. It is these disagreements in methods and the resulting uncertainties in both the actual CO_2 flux and the specific mechanisms responsible for the flux, which require a comparison of methods and an analysis of the physical processes controlling the flux of gas across the air-water interface [see also *Fairall et al.*, 2000].

[4] In this paper, we report measurements of two lakes in which water-atmosphere fluxes of CO_2, water vapor, and energy were measured during periods with convective mixing of the epilimnion: (1) during a cross-calibration experiment over Toolik Lake (Alaska), where floating chamber and EC flux measurements were simultaneously performed over four days in late July 1995 and on one day in July 1994; and (2) in a subsequent field experiment in September 1998 over Soppensee, a small lake in Switzerland. For comparison, fluxes were also calculated from a wind based model [*Cole and Caraco*, 1998] developed for small lakes and from a surface renewal model which incorporates turbulence at the air-water interface [*MacIntyre et al.*, 1995]. Flux measurements from both sites revealed a complex pattern of gas flux which appears to be mainly a result of the interplay of physical and biogeochemical processes occurring in the atmosphere and in the lakes. During the study at Soppensee, wind speeds never exceeded 3 m s^{-1}. This data set allows us to examine the processes regulating gas flux in the absence of strong wind and with conditions of small waves.

[5] A more comprehensive set of physical measurements was obtained during the Soppensee experiment than at Toolik Lake. Hence the Soppensee experiment is described first as it provides insight into the Toolik Lake results from 1995. The 1994 measurements at Toolik Lake were so short that they are only included in this paper for the purpose of validation.

2. Sites, Data, and Methods

2.1. Sites

2.1.1. Toolik lake

[6] Toolik Lake (68° 37.91′ N, 149° 36.32′ W, 719 m a.s.l.) is a small lake north of the Brooks range in Alaska. For the past 25 years it has been the focus of arctic studies [*O'Brien et al.*, 1997], being the site of the U.S. Arctic Long-Term Ecological Research (LTER) station. Toolik Lake has a surface area of 1.5 km^2, an average depth of 7 m, and a maximum depth of 25 m [*O'Brien et al.*, 1997]. The main inlet to the lake provides an inflow of $125 \cdot 10^3$ m^3 d^{-1}, which is 71% of the total inflow [*O'Brien et al.*, 1997] (measured between 13 May and 31 August 1980). The high dissolved organic carbon (DOC) concentrations (≈5–7 mg L^{-1}) reduce penetration of irradiance in the water with a typical attenuation coefficient of 0.5 m^{-1}.

[7] Dissolved inorganic carbon (DIC) fluxes in Toolik Lake are dominated by river inflow and outflow, groundwater inputs, and gas evasion to the atmosphere [*O'Brien et al.*, 1997]. The river and groundwater inputs are supersaturated in CO_2 with respect to the atmosphere, and gas evasion averaged ≈420 mg C m^{-2} d^{-1} during the open water period of the year of about 100–120 days [*Kling et al.*, 1991, 1992].

2.1.2. Soppensee

[8] Soppensee is a small holomictic eutrophic lake located 20 km northwest of Lucerne, Switzerland (47° 05.46′ N, 8° 05.00′ E, 596 m a.s.l.). It is about 800 m long and 400 m

wide with a surface area of 0.25 km^2, and an average and maximum depth of 12 m and 27 m, respectively. The lake drains a 1.6 km^2 catchment [*Lotter*, 1989; *Gruber et al.*, 2000]. Soppensee has an outstanding record of varved sediments that have allowed the reconstruction of the environmental history [*Lotter*, 1989] back to the last ice age. The varved sediments indicate very stable conditions of the sedimentation cycle and of the redox conditions. A strong thermal stratification generally develops in summer with a rather constant epilimnion at about 3–4 m depth, and anoxic conditions in the bottom waters [*Gruber et al.*, 2000].

[9] A mass balance of the carbon cycle computed by *Gruber et al.* [2000] indicates that most of the inflow comes from groundwater which is, similar to Toolik Lake, supersaturated with respect to atmospheric CO_2. The modeled annual CO_2 efflux from Soppensee amounts to about 164 mg C m^{-2} d^{-1} [*Gruber et al.*, 2000]. While Soppensee itself is surrounded by a narrow band of reed and forest vegetation, the largest fraction of the catchment area is intensely used for agricultural purposes.

[10] In autumn, the season during which our field measurements were taken, the surface inflow to and outflow of DIC from Soppensee is almost zero, and the $CaCO_3$-rich ground water is the main factor for the supersaturation of the surface waters with DIC. The DIC concentration in the lake is rather constant both in the epilimnion and the hypolimnion, and it increases in the transition zone of the metalimnion [*Gruber et al.*, 2000].

2.2. Eddy Flux Measurements

2.2.1. Instrumentation

2.2.1.1. Floating Platforms

[11] At Toolik Lake, for the 1995 experiment (27–31 July), we moored a platform near the center of the lake to have equally good fetch for the EC system of at least 200 m in all directions. The platform measured 2.42 × 6.10 m^2, and consisted of two elements of equal size that were attached to each other with a hinge in the middle. The surface of the platform was 0.38 m above the lake surface when all equipment was loaded on the float. In 1994 (14–15 July), the instruments were mounted on the northern lake shore, which required that data with mean wind direction from the land were excluded from the analysis.

[12] At Soppensee (21–23 September 1998), we used a much larger and more stable platform to further minimize the influence of the oscillations observed in the time series recorded at Toolik Lake. The size of this platform was 5 × 7 m^2, and it was mounted on two boats. Thus the surface of the platform was typically 0.80 m above the lake. The positioning of the platform was more critical than at Toolik Lake because of the smaller size of Soppensee, and the trees around the lake, representing significant roughness elements that increase turbulence over the lake. The optimum mooring location was determined from ten years of wind data from three automatic weather stations within 18 km distance from the site. The expected fetch determined by the distance to the shore was ≈440 m in the best case (with winds from the prevailing wind direction 300°), and ≈125 m in the worst case.

2.2.1.2. Eddy Covariance Systems

[13] The two EC systems used at both sites were completely different and will therefore be described individually. At Toolik Lake, the set-up consisted of an ATI 3-D sonic anemometer and thermometer (Applied Technologies, Inc., Boulder, Colorado, United States, model SAT-211/3Vx) operating at 10 Hz in 1994 and 20 Hz in 1995. Measurement height was 1.50 m and 1.62 m above the surface in 1994 and 1995, respectively. A closed-path infrared gas analyzer (IRGA) performed CO_2 concentration measurements. A fast LI-COR 6262 instrument (LI-COR, Lincoln, Nebraska, United States) was used in 1994, providing 5 Hz time resolution, while in 1995 a LI-COR 6252 operating at a 1-s time resolution was used. A brass tube (4 mm inner diameter, 1 m long, wrapped with polyurethane insulation and reflective foil tape to minimize rapid temperature fluctuations in the air stream) was positioned at a distance of 15 cm from the center of the sonic anemometer's measuring volume. The air-sampling tube was connected to the gas analyzer by ≈2.5 m of polypropylene tubing (3.2 mm inner diameter, Bev-a-line), and air was drawn through the system by a diaphragm vacuum pump at 8–9 L min^{-1}. This rate was adequate to maintain turbulent flow in the sampling tube and reduce limits on system bandwidth due to the volume (11.9 cm^3 of the gas analyzer cell; *Leuning and King* [1992], *Suyker and Verma* [1996], and *Leuning and Judd* [1996]). A 1-m vacuum hose between the IRGA and the pump was used to reduce the effect of high-frequency pressure fluctuations. The IRGA was calibrated with zero air and a calibration gas standard (402 ppm, Matheson Gas Products, Montgomeryville, Pennsylvania, United States) under ambient conditions. The values were cross-validated against a LI-COR 6262 instrument; then, the LI-COR 6252 was attached to the pump, and the span was adjusted in such a way that the concentration readings matched the LI-COR 6262 concentration readings. Finally, all data were post-calibrated for the present analysis with independent concentration measurements performed using a gas chromatograph (for details, see *Kling et al.* [2000]). CO_2 concentration and flux values were multiplied by 1.078 in this post-calibration step. This procedure was necessary because the LI-COR 6252 instrument has no pressure correction built in and therefore shows too low concentrations when air is pulled through the instrument at the required rate.

[14] At Soppensee, we used a Solent HS 3-D research grade sonic anemometer and thermometer (Gill Instruments Ltd., Solent, U.K.) that operates at 100 Hz and provides error-checked averaged measurements at 20 Hz temporal resolution. This instrument also has a built-in inclinometer, which allowed for the identification of any time period within which the float had changed its position. However, the slow response of the inclinometer did not allow for instantaneous corrections of high-frequency oscillations of the float. For CO_2 and H_2O measurements we used a NOAA open-path IRGA [*Auble and Meyers*, 1992], which was modified to avoid moisture in the housing and to reduce the internal noise level using a 63 μF capacitor between signal and ground. The chopper wheel rotation speed was set to 30 Hz in order to provide the highest possible temporal resolution. The instrument was mounted 2.80 m above lake surface, at a horizontal distance of 0.74 m from the center of the sonic anemometer's sensor array. Neither pump nor tubing were needed for this open-path instrumental set-up. The IRGA was calibrated with a CO_2-free gas and three CO_2

gas standards (318, 415 and 559.4 ± 2 ppm; Carbagas, Liebefeld, Switzerland). The H_2O channel was calibrated with a dew point generator in the Paul Scherrer Institute (Villigen, Switzerland), using seven dew point temperatures between 0.85 and 18.81°C.

2.2.1.3. Additional Measurements From Toolik Lake

[15] Net radiation measurements (R_n) were performed with a Fritschen-type net-radiometer [*Fritschen*, 1960] from Radiation and Energy Balance Systems (REBS, Seattle, Washington, United States, model Q*6) and mounted at 0.41 m above lake surface. A Davos-type net pyrradiometer [*Ohmura and Schroff*, 1983] from Swissteco (model S-1, Oberriet, Switzerland) was mounted at 1.62 m height. The REBS instrument was intercalibrated with the Swissteco reference instrument in the field at Happy Valley (69°07′ N, 148°50′ W) on 18–19 June 1995, and new calibration factors for the REBS instrument were derived and used throughout the study. Because of unequal response to shortwave and long-wave radiation of the REBS instruments [*Field et al.*, 1992; *Whiteman et al.*, 1989], different calibration coefficients were used for $R_n \geq 0$ and $R_n < 0$. The Davos-type reference instrument was factory-calibrated before (19 October 1990) and after (16 September 1995) the intercalibration experiment at Happy Valley.

[16] Air temperature and moisture at EC height was measured with a Väisälä-type thermometer/hygrometer (Campbell Scientific, Logan, Utah, United States, model HMP35C). At 0.39 and 0.46 m above the lake surface, air temperature and moisture were measured with a home-built aspirated psychrometer, which uses the AD592 integrated circuit temperature sensor (Analog Devices, Inc., Norwood, Massachusetts, United States). One of the sensors was kept moist with a wick. The psychrometer sensors were calibrated at 0°C over a crushed ice-water bath and at 30°C in a warm water bath. Water temperature was measured at depths of 0.005, 0.04, 0.14 and 0.34 m with platinum resistor sensors (REBS model STP-1). The wind profile was measured with hot wire anemometers (TSI, Inc., St. Paul, Minnesota, United States, model 8470) at 0.66, 1.02, 1.62 and 2.38 m a.g.l. with a ±3% accuracy in the range 0–5.0 m s^{-1}.

[17] Radiation and meteorological sensors were polled every 20 s by a data logger (model 21x, Campbell Scientific, Logan, Utah, United States) and averages were recorded every 6 min.

2.2.1.4. Additional Measurements at Soppensee

[18] The CO_2 concentration gradient was measured between EC height and 0.30 m above the water surface with a LI-COR 6262 IRGA. The IRGA was run in absolute mode and the inlets were switched by an automatic valve every 30 s. Data from the first 10 s of each cycle were discarded in order to allow the sample cell to adapt to the change in concentration. The sample flow rate was 5 L min^{-1}.

[19] Net radiation was measured with a Swissteco net pyrradiometer (model S-1; Oberriet, Switzerland) at 0.42 m above the water surface in order to minimize the influence of the floating platform. The thin domes of the instrument were inflated with pressurized dry air, and the outer surface was kept dry by a steady air current over the domes. The sampling cycle of the CO_2 concentration gradient was controlled by a data logger (model CR10X, Campbell Scientific Ltd., Loughborough, UK) which also collected the data of the IRGA and the net pyrradiometer, thereby using an internal averaging interval of 5 min.

[20] Additional measurements were obtained from an Aanderaa Instruments weather station (Bergen, Norway) equipped with a data logger and the following sensors: air temperature and relative humidity in a radiation shield and cup anemometers at 0.5, 1, 2, and 5 m above lake surface; wind direction, buoy orientation, upward looking pyranometer and pyrradiometer sensors at 5 m; and downward looking pyranometer and pyrradiometer sensors at 0.5 m. A chain of thermistors assembled from Richard Brancker Research (Ottawa, Canada) TR-1000 self-contained temperature logging units with 0.002 K resolution (absolute accuracy ±0.05 K) at depths of 0.5, 2.5, 4.5, 6, 7, 8, 9, 10, 12, 17, and 25 m measured temperature in 2-s intervals. A Nortek (Sandvika, Norway) 25° beam angle high resolution acoustic Doppler current profiler (ADCP) operating at 1.5 MHz (resolution 0.1 mm s^{-1}; sampling frequency 0.5 Hz) was employed to measure water velocities between 3.3 and 7.2 m depth using 40 vertical bins with 0.1 m spacing. A SeaBird (SBE-Electronics, Washington, D. C., United States) SBE 9/11 CTD profiler with an FP-07 fast response temperature probe (response time ≈15 ms at 0.1 mK resolution) was employed in a cable-constrained uprising mode at ≈0.08 m s^{-1} velocity. Data were collected at 96 Hz.

2.2.2. Computations

[21] The turbulent energy and CO_2 fluxes in the vertical direction above the lake surface were derived from the covariances of the vertical wind speed w and the energy content or CO_2 concentration c,

$$F_c = \overline{w'c'}. \quad (1)$$

F_c is the vertical turbulent flux of entity c, the overbar denotes a temporal average (30 min were used for Toolik Lake data, 5 min for Soppensee data according to section 3.1), and primes denote the instantaneous turbulent fluctuations relative to its temporal mean, e.g., $w' = w - \bar{w}$. We use the micrometeorological sign convention with positive values for w and vertical fluxes if they are directed away from the surface toward the atmosphere, and negative values if the direction is toward the surface. Ground heat flux is taken positive when directed from the surface to the water body, and radiative fluxes are positive when directed toward the surface.

[22] The heat exchange between the lake water and the atmosphere was computed from the CTD temperature profiles that were measured at 30-min intervals and then filtered over 6 consecutive profiles to eliminate apparent fluxes due to internal wave motion.

2.2.3. Data Processing

[23] Processing of the raw EC data included the following steps: (1) removing spikes in the ATI sonic anemometer data from Toolik Lake using an iterative two-sided filter that removes outliers outside the local 30-min average ±3σ (where σ is the standard deviation; the Solent sonic anemometer employed at Soppensee did not require this treatment because its software does error checking and elimination internally); (2) quality check of 1-min averaged values of mean quantities and fluxes; (3) coordinate rotation of u, v and w wind components to align coordinate system with the stream lines of the 30-min averages [e.g., *Zeman*

and Jensen, 1987; *McMillen*, 1988; *Kaimal and Finnigan*, 1994, pp. 235–239]; (4) determining time lag values for H_2O and CO_2 channels using a cross-correlation procedure that finds the maximum absolute correlation within a time lag window of $0.5 \leq \tau \leq 2.0$ s for each 30-min segment of raw data; (5) de-trending sonic temperature, H_2O and CO_2 channels using a linear trend elimination procedure (see *Rannik and Vesala* [1999] for a discussion of linear detrending versus auto-regressive filtering); (6) computing mean values and turbulent fluxes; (7) calibration of H_2O and CO_2 fluxes to account for damping and high frequency losses using the *Eugster and Senn* [1995] cospectral correction model (see *Horst* [2000] for the validity of this approach and *Massman* [2000] and *Massman and Lee* [2002] for a similar approach); (8) correction of H_2O and CO_2 fluxes to account for the effect of concurrent density fluctuations according to *Webb et al.* [1980].

[24] For the final analysis, only those flux measurements were used which were obtained during periods where the momentum flux was directed toward the surface. If the momentum flux is not downward, then all EC fluxes measured under such conditions are not expected to be a direct function of the local surface exchange processes. This criterion eliminated 28% and 6% from our Toolik Lake and Soppensee data sets, respectively.

2.3. Floating Chamber Measurements

2.3.1. Instrumentation

[25] Gas flux measurements were taken eight times during the sampling period at Toolik Lake by means of a floating chamber. The clear Plexiglas chamber had an area of 0.2 m^2 and a headspace volume of ≈30 L. From the headspace at least four headspace gas samples were taken during the 60-min deployment. The gas samples were analyzed on a gas chromatograph with a thermal conductivity detector. Water samples were also taken during chamber employments, and analyzed for dissolved CO_2 content on a gas chromatograph after a headspace equilibration (see *Kling et al.* [2000] for further details).

2.3.2. Computations

[26] Gas exchange at the water surface was estimated from the floating chamber using a time series of CO_2 measurements in the chamber headspace. The fundamental model of the change in gas concentrations (C) over time (t) in the headspace is given by

$$dC/dt = -k(C_{\max} - C), \tag{2}$$

where k [s^{-1}] is the gas exchange rate, and $C_{\max}$ is the maximum concentration in the water; as C approaches $C_{\max}$, dC/dt approaches zero. The relationship

$$\ln(dC/dt) = \ln k + \ln(C_{\max} - C_0) - kt, \tag{3}$$

involving the initial concentration in the headspace C_0, was fitted to the measurements using the least-squares technique. The variance in gas flux was taken as the standard error of the model estimate of $\ln k + \ln (C_{\max} - C_0)$.

[27] Overall fits to the model were good ($r^2 > 0.91$) if dC/dt was large (3 samples). However, in cases where dC/dt was small (5 samples), the equation produced poor fits to the data, and estimates of the slope and intercept were not significantly different from zero (at $p < 0.05$). In these cases, a simple linear relationship of $C(t) = \alpha_0 + \alpha_1 t$ provided a good fit (r^2 range of 0.85–0.98), and the slope α_1 of this relationship ($\alpha_1 = dC/dt$) was used to estimate the change in gas concentration during the chamber employment. Overall gas flux (mg C m^{-2} d^{-1}) was obtained by correcting the dC/dt values in the chamber headspace for the chamber volume and surface area. The variance in gas flux was taken as the standard error of the model estimate of α_1, which was corrected for chamber volume and surface area.

[28] In two cases the concentration of CO_2 in the chamber decreased from one headspace measurement to another (≈10–15 min apart); although this indicates an uptake of CO_2 by the lake water, the overall flux during these two employments (≈60 min each) showed a net evasion from the lake to the atmosphere.

[29] Gas flux was also estimated at Toolik Lake from wind speed and measured differences between concentrations of CO_2 in the surface water and in the atmosphere [*Cole and Caraco*, 1998]. Here we refer to this approach as the boundary layer model (BLM). Convective mixing in the water is not explicitly included in this model. We also estimated gas flux using a surface-renewal model (SRM) which includes both the effects of wind speed and heat loss at the air-water interface in its formulation [*Crill et al.*, 1988; *MacIntyre et al.*, 1995]. The turbulent velocity scales due to wind u_{*w} and heat loss w_* (the penetrative convection velocity scale according to *Imberger* [1985] and *Deardorff* [1970]) were obtained from a surface energy budget calculated as done by *MacIntyre et al.* [2002] using surface irradiances and wind speed obtained by the meteorological station. This approach is based on *Imberger* [1985] with the computation of heat flux at the air-water interface including the penetration of irradiance into the mixed layer and below. Consequently, it accurately calculates the heating and cooling of the surface mixing layer in which turbulent mixing occurs. The gas transfer velocity k_{SRM} was calculated using the small eddy version of the surface-renewal model, $k_{\mathrm{SRM}} Sc^{1/2} = c_2 u_{*w} Re_t^{-1/4}$, where k_{SRM} is the gas transfer velocity, Sc is the Schmidt number, c_2 is an empirical coefficient (0.56), u_{*w} is the turbulent velocity scale, and Re_t is the turbulent Reynolds number. The depth of the surface mixing layer is the turbulent length scale. It is generally demarcated by temperature differences as small as 0.01°C. Only one temperature profile was measured at Toolik Lake during the field campaign, and it showed the depth of the upper mixed layer was 3 m. The combination of this profile, the surface meteorological data, and subsequent time series studies of temperature at Toolik Lake from 1998–2000 provide a basis for estimating the depth of the mixing layer during a variety of meteorological conditions at Toolik. During the initial period in which air temperatures were much cooler than water temperatures, we used 3 m. During the second half of the experiment, when the air-water temperature difference was less, we used a depth of 1 m. When air temperatures exceeded lake temperatures as determined by the thermistors in the upper 0.34 m, we let the mixing depth be 0.1 m. At Soppensee, we used a mixing depth during convective conditions of 6 m, a depth based on profiles of temperature gradients. During heating periods, we used a mixing depth of 1 m. These values must be considered as estimates representing relative conditions

within the measurement period and thus provide an understanding of the physical processes occurring in the lake. Additional computational details are presented by *MacIntyre et al.* [2001, 2002].

3. Data Quality Assessment

3.1. Frequency Analyses

[30] Spectral and cospectral analyzes were used to control the proper operation and the time response of the individual instruments and the flux measurements, respectively. The *w* and *c* spectra at Soppensee exhibited throughout a pattern corresponding to the expected idealized spectra (Figure 1). The typical $f^{-2/3}$ slope of the inertial subrange started at natural frequencies beyond approximately 1 Hz, which was generally well below the Nyquist-frequency of the measured time series which was 10 Hz (see example spectra in Figure 1). Traces of white noise in the spectra begin to be relevant at $f > 4$ Hz (occasionally at $f > 1$ Hz). The H_2O channel of the IRGA experienced a certain damping loss at high frequencies which was much less pronounced in the CO_2 channel of the same instrument. This damping is a result of the additional 63-μF capacitor signal filter and the internal anti-aliasing filter of the sonic anemometer's analog input channels. The overall damping constant of this set-up was 0.30 s. This damping is not considered critical for our flux measurements, since its behavior is well understood and was corrected for using the approach by *Eugster and Senn* [1995; see also *Horst*, 2000].

[31] Difficulties in measuring very small CO_2 fluxes, however, still remain. In addition to instrumental limitations to resolve small fluctuations in CO_2 concentration, the *Webb et al.* [1980] density flux can be much larger than the true flux of CO_2 [e.g., *Leuning et al.*, 1982]. *Webb et al.* [1980] found that the true flux F_c of a scalar quantity is the measured flux F_{raw} of that quantity plus an additive density

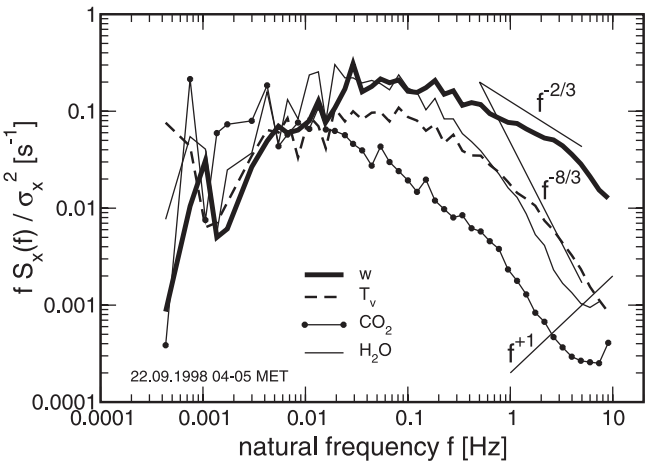

Figure 1. Power spectra of a 1-hour time segment of eddy covariance data collected at Soppensee between 4 and 5 hours CET on 22 September 1998. The theoretical slopes of the inertial subrange are also given for undamped ($\propto f^{-2/3}$) and damped ($\propto f^{-8/3}$) spectra. High-frequency noise only appears in the spectrum of H_2O and CO_2 at frequencies >7 Hz. The sonic anemometer measurements do not show any signs of high-frequency noise.

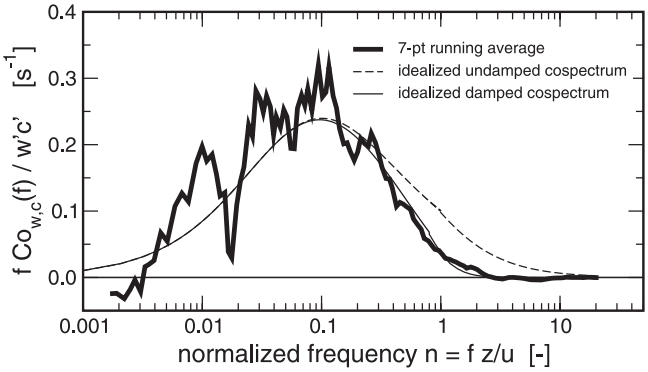

Figure 2. CO_2 flux cospectra from Soppensee during periods without convection in the lake. Composite of three 1-hour cospectra (bold line; DOY 265, 12–13 and 15–17 hours CET), and idealized undamped (thin dashed line) and damped cospectra (thin solid line; damping constant 0.30 s; see *Eugster and Senn* [1995]).

flux F_ρ, $F_c = F_{raw} + F_\rho$, where F_ρ is a function of the sensible and latent heat fluxes. This is certainly a problem for open path IRGAs such as the one used at Soppensee [see *Leuning and Judd*, 1996], but to a lesser extent for the closed path IRGA used at Toolik Lake. Using the formula suggested by *Leuning and Moncrieff* [1990] we estimate that the tubing used at Toolik Lake reduced temperature fluctuations by a factor 40 such that the *Webb et al.* [1980] density flux contribution is quite small, but nonzero because of moisture fluctuations. In cases where F_{raw} is small the sign of F_c could switch when F_ρ is added. This was the case during 10.9% and 30.8% of the time at Toolik Lake and Soppensee, respectively. We used this criterion to estimate the 95% confidence intervals for CO_2 fluxes that might not significantly differ from zero. This range was −0.0009 to 0.0018 mg C m^{-2} s^{-1} at Toolik Lake and 0.0002 to 0.017 mg C m^{-2} s^{-1} at Soppensee. Note that in the latter case we measured during a period where the water remained warmer than the air at all times, such that $F_\rho > 0$. The signal-to-noise ratio of the IRGAs in use was less problematic (median values of 92.5 and 172 were found at Toolik Lake and Soppensee, respectively).

3.1.1. Determination of Averaging Time for Soppensee Data

[32] The cospectral analyses showed good correspondence with the idealized cospectra (Figures 2 and 3). The idealized cospectra scale with normalized frequency *n*, where $n = f \cdot z/\bar{u}$ [e.g., *Panofsky and Dutton*, 1984] is derived from the natural frequency *f*, the measurement height *z*, and the mean horizontal wind speed $\bar{u}$. This good agreement was found in all latent heat flux cospectra and the CO_2 flux cospectra during periods with low variability of the CO_2 flux. The only exceptions were found in the case of CO_2 flux during periods with high variability, although latent heat flux cospectra were almost ideal (Figure 3). During such periods the lower frequencies of the cospectrum were disturbed by low-frequency variations at $n < 0.0125$ (Figure 4). By using Taylor's frozen turbulence hypothesis and under the assumption of local stationary turbulence conditions, this frequency scale can be translated into a wave number scale, $\kappa_1 = 2\pi f/\bar{u}$ [see *Kaimal and*

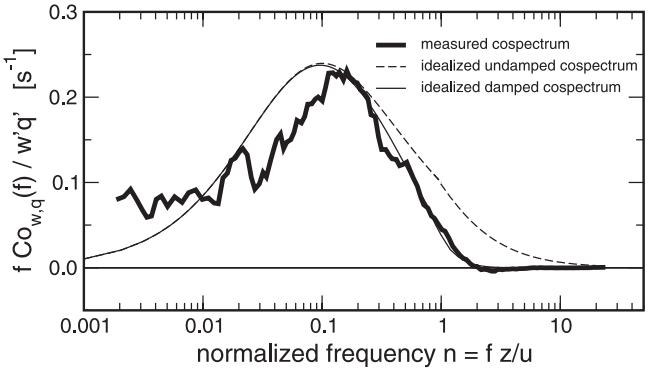

Figure 3. H_2O flux cospectra from Soppensee during periods with largest CO_2 efflux from the lake, composite of three 1-hour length data segments (bold line; DOY 265, 01–02 and 20–21 hours CET; DOY 266, 21–22 hours CET). The composite cospectrum closely follows the idealized damped curve at frequencies $n > 0.2$, indicating the high quality of the turbulent flux measurements.

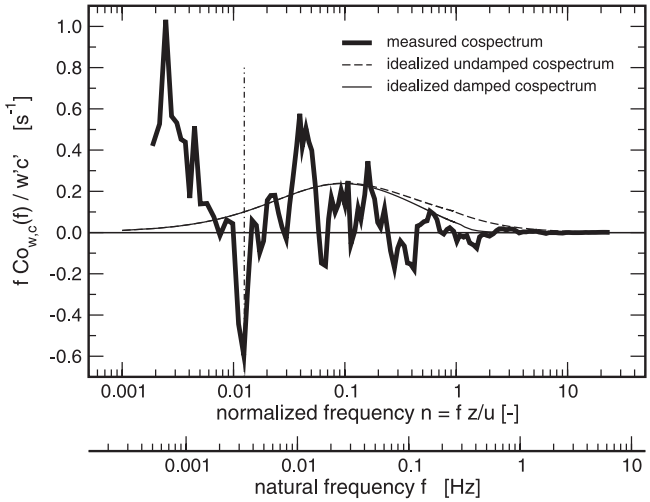

Figure 4. As in Figure 3 but for CO_2 flux. Vertical dash-dotted line indicates the cutoff of the 5-min high-pass averaging filter, which eliminates all fluctuations to the left of that line.

Finnigan, 1994, p. 60]. To convert κ_1 into spatial wavelength scale, we used the relationship $\lambda = 2\pi/\kappa_1$ [see *Panofsky and Dutton*, 1984, p. 74], yielding $\lambda = z/n$, where λ is the spatial wavelength in units of m. With $z = 2.8$ m, λ of this low-frequency contribution is on the order of 225 m, indicating that lower frequencies are most likely affected by the respiration occurring on land, a process which cannot directly be related to the CO_2 exchange process across the lake surface. Therefore we filtered the Soppensee fluxes by truncating the computation of the covariance at $f = 0.0033$ Hz ($n \approx 0.0125$; dash-dotted vertical line in Figure 4) in order to eliminate the contribution of CO_2 flux that most likely originates from the land surrounding the lake. This was done by averaging covariances over 5-min intervals, which were further block-averaged to 30-min values. It should however be noted that this procedure only captures ≈92% of the flux expected over ideal terrain as can be determined by integrating the *Kaimal et al.* [1972] cospectra from Kansas.

[33] It is remarkable that in contrast to the CO_2 flux measurements (Figure 4), the vapor fluxes, measured with the same combination of instruments, were nicely obeying the idealized cospectrum during these periods (Figure 3).

3.1.2. Determination of Averaging Time for Toolik Lake Data

[34] In the case of Toolik Lake we used standard 30-min averaging periods. The influence of the surrounding land surface on the CO_2 flux measurements (see Figure 5) appeared to be less problematic than at Soppensee. The low-frequency variation seen in Figure 5 is partially eliminated from the covariance computations by using standard 30-min averaging periods. It is expected that the clear gap between $0.001 < n < 0.035$ separates flux contribution from the land (lower frequencies) from the ones that are related to the lake surface exchange.

3.1.3. Oscillations From Floating Platforms

[35] In contrast to the measurement set-up on Soppensee, the floating platform on Lake Toolik was much smaller. Therefore the oscillation of the float due to surface waves is clearly visible in the wind velocity spectra (Figure 6a). On average, the extra variance introduced in the vertical velocity time series is on the order of 6% of $\overline{w'^2}$ and restricted to a narrow band of frequencies $0.7 < f < 1.2$ Hz (Figure 6a). Although significant, this oscillation does not strongly influence the cospectrum of the flux measurements (Figure 6b). Therefore we believe that there is no need for a special flux correction to eliminate the traces of this oscillation. In the case of the Soppensee data, the typical wind speed was clearly lower than over Toolik Lake, and the floating platform was more rigid and larger, which reduced the effect of oscillations to the variation normally observed in spectral data. The motion contamination due to the gyroscopic effects described by *McGillis et al.* [2001] appear to be negligible because of the relatively small perturbations in the lake compared to the open ocean.

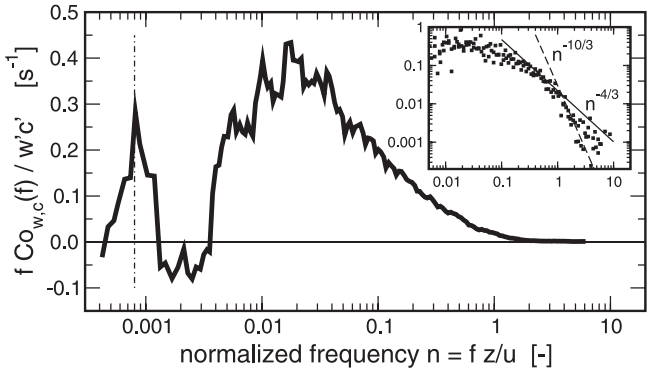

Figure 5. CO_2 flux cospectra from Toolik Lake during periods without convection in the lake. Composite of four 1-hour cospectra (DOY 212, 00–01, 02–03, 04–06 ADT). Fluxes that are computed over standard 30-min intervals integrate all information to the right of the vertical dash-dotted line. The inset shows the details of the inertial subrange slope with the expected undamped slope (solid line) and the damped slope (dashed line). Average $z/\bar{u}$ was 1.49 s.

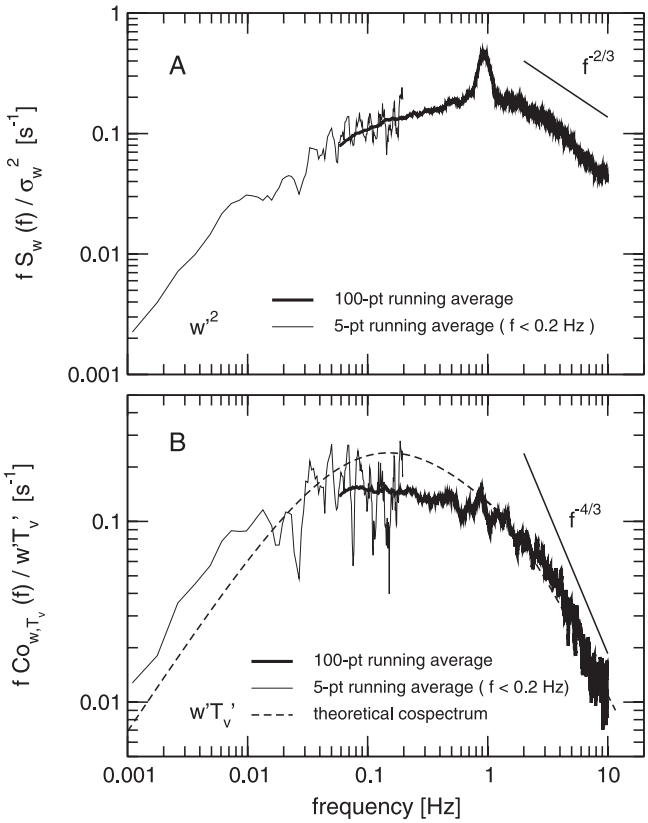

Figure 6. Influence of the float oscillation on (A) the variance of vertical wind speed, and (B) the covariance $\overline{w'T_v'}$ (turbulent sensible heat flux). Data are from 27 July 1995, 18–19 hours local time at Toolik Lake (100-point running averages and 5-point running averages for the low-frequency part). The variance added to $\overline{w'^2}$ is restricted to the narrow frequency band 0.7–1.2 Hz, adding ≈6% to the total variance. However, this float oscillation does not dramatically influence the covariance or flux measurements (Figure 6b). The theoretical slope of the inertial subrange is given by the separate line.

3.2. Energy Budget Closure

[36] Good energy budget closure is generally considered an indication of good quality flux measurement [*Baldocchi*, 1994]. At Soppensee, the heat exchange across the water interface was determined by three independent methods: (1) as the residual term $G_{\text{EB-closure}} = R_n - H - LE$ as determined from the micrometeorological measurements, where R_n is net radiation, and H and LE are turbulent sensible and latent heat fluxes, respectively; (2) G_{micT} determined from the microstructure temperature profile in the epilimnion including the penetration and entrainment zone in the depth range 3.3–7.3 m; and (3) the heat exchange $G_{\text{T-chain}}$ determined from the temperatures of the array of thermistors that were bin averaged for 5-min intervals and then filtered over ±4 hours. In theory we expect $G_{\text{EB-closure}} = G_{\text{micT}} = G_{\text{T-chain}}$ since they simply represent the same variable determined in three independent ways.

[37] Figure 7 depicts the energy budget components for the time period where measurements from all instruments overlap. Here we use G_{micT} as a reference, against which other methods should be tested. The general agreement between G_{micT} and $G_{\text{EB-closure}}$ is excellent, thereby confirming the validity of the EC method. The average difference between $G_{\text{EB-closure}}$ and G_{micT} was <10 W m^{-2}, with a slight bias toward $G_{\text{EB-closure}} > G_{\text{micT}}$. The EC turbulent flux measurements do not include advective flux components, which might be significant at this location and which may well be of the same order of magnitude as the difference between G_{micT} and $G_{\text{EB-closure}}$.

[38] Overall, the energy budget data in Figure 7 indicate that the EC flux measurements are of high quality. In addition to the quality control performed by using frequency analyzes, the agreement of the energy budget estimates also indicates excellent performance of the EC instruments.

4. Soppensee CO_2 Exchange

[39] Our measurements from Soppensee indicate the existence of two distinctly different regimes of CO_2 exchange,

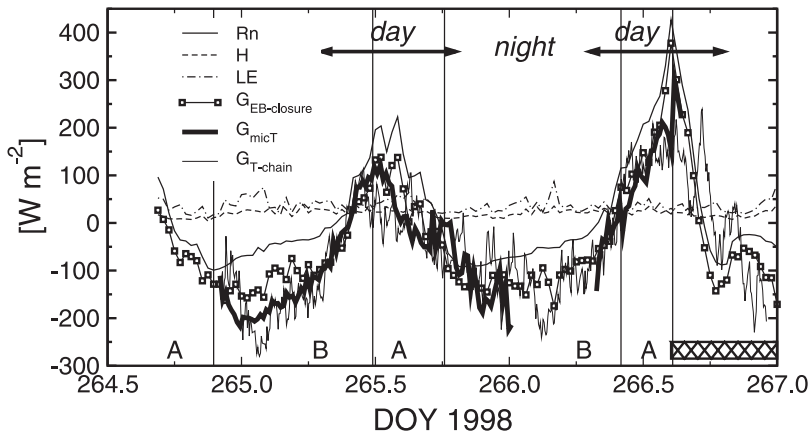

Figure 7. Energy fluxes observed at Soppensee, and agreement between methods. Rn: net radiation; H and LE: sensible and latent heat fluxes measured with the eddy covariance method; $G_{\text{EB-closure}}$: surface heat exchange with the water body determined as the residual term $G_{\text{EB-closure}} = \text{Rn} - \text{H} - \text{LE}$, using half-hourly averages; G_{micT}: surface heat exchange determined from the temperature profiler data; $G_{\text{T-chain}}$: surface heat exchange determined from the thermistor chain data.

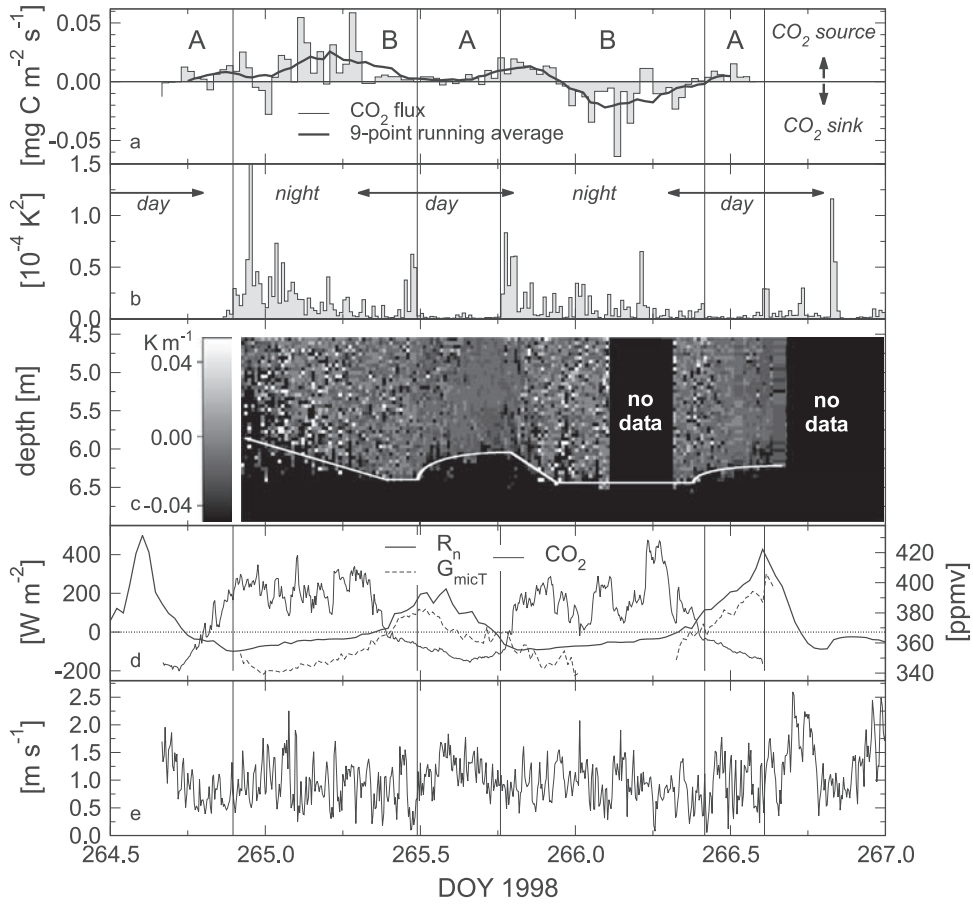

Figure 8. Eddy covariance CO_2 flux (a) measured above the surface of Soppensee (5-min fluxes block averaged over 30-min intervals) and independent measurements of: (b) the 15-min variance of water temperature at 4.4 m depth; (c) temperature gradient in the depth range 4.5–7.0 m as measured with the CTD profiler, bin averaged upon 5-cm bins; (d) net radiation (bold line), G_{micT} from Figure 7 (dashed line), and ambient CO_2 concentration (thin line); and (e) horizontal wind speed at 2.80 m height. The gray shade levels in Figure 8c are proportional to the vertical temperature gradient in K m^{-1} (negative numbers indicate decreasing temperature with depth), and the white line corresponds to the lower boundary of the convective aquatic layer (B periods), and of the remnant mixed layer (A periods), respectively. The surface water temperatures (not shown) varied between 15.3 and 16.9°C. Letter A denotes times with low variance of the epilimnion temperature at 4.4 m depth, while B denotes times with substantially higher variance.

illustrated by A and B periods in Figure 8. The A and B periods reflect the expected differences between calm conditions (A) with warmer atmosphere and thus stably stratified surface waters, compared to convective conditions (B) with colder air and the convective mixing of the epilimnion. A and B periods thus reflect the stratification in the lake, not in the air.

[40] The A periods exhibited relatively smaller CO_2 fluxes with very little variability (Figure 8a). The resulting net flux was generally in the direction from the water to the atmosphere, although individual 30-min flux averages (derived from 5-min covariances; compare section 3.1) showed either a zero net CO_2 flux, or even a small CO_2 uptake. Concurrent independent measurements of TR-1000 temperature variation at 4.4 m depth (Figure 8b) and microstructure profiler temperature gradients (Figures 8c and 9) confirm the calm and stratified conditions in the water during the A periods (further details on temperature profiles in the lake will be presented by *Jonas et al.* [2003].

[41] Epilimnetic temperatures had a high variance during B periods (Figure 8b). In addition, the CTD profiler showed that temperature gradients occurred frequently throughout the water column during these times (Figures 8c and 9). The presence of temperature gradients which reverse sign frequently, is indicative of turbulent mixing in the water column [*Imberger*, 1985]. R_n was negative during B periods, and wind speeds were low. Heat fluxes out of the mixed layer occurred during B periods. Turbulent velocity scales in water due to heat loss (w_*) are four times larger than those due to wind forcing (u_{*w}). Hence the mixing was driven by heat loss at the air-water interface. During both nights (days 264/265 and 265/266) radiation fog formed which reduced long-wave radiative losses dramatically during the second half of the night. The gas transfer velocities (data not shown) calculated by the surface renewal

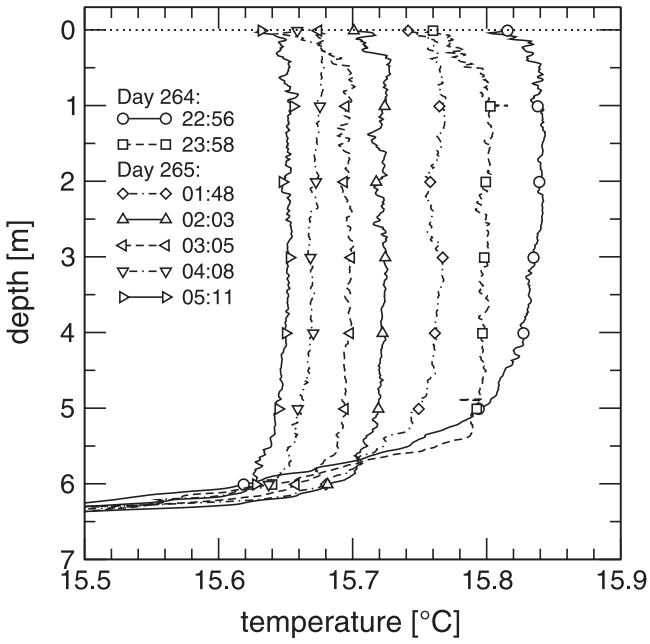

Figure 9. Dynamics of the temperature stratification indicating convection during the night of day 264/265. Shown are calibrated hourly averaged temperature profiles measured with the FP-07 fast response probe on the CTD profiler. Each profile shown represents an average over four profiles taken at 15-min intervals. See *Jonas et al.* [2003] for further details.

model (k_{SRM}) are 2.5 times larger than those due to the wind based boundary layer model (k_{BLM}) during times of heat loss and further are sensitive enough to indicate that gas flux would be suppressed during heating periods.

[42] The variability in turbulent CO_2 flux in the atmosphere during such convective periods is closely coupled with the temperature variation in the mixed layer of the epilimnion (Figure 8b). Convective mixing not only increases the vertical transport of dissolved CO_2 in the mixed layer, but also leads to enhanced turbulence at the air-water interface, thereby enhancing gas transfer between lake and atmosphere.

[43] The observed short-term flux densities were much larger during convective than calm periods on DOY 265. Maximum CO_2 loss from the lake was observed after midnight until 7 hours local time. The mixed layer deepened during this period. During the second night only the first few hours experienced CO_2 efflux from the lake, while a clear uptake was observed during the second part of the night. The mixed layer did not deepen the second night. Continued deepening of the mixed layer appears necessary to maintain outward fluxes of CO_2 at Soppensee. Enhanced fluxes occurred at times when k_{SRM} was elevated.

[44] Figure 10 illustrates turbulence in the upper mixed layer with and without mixed layer deepening due to penetrative convection. The conditions during penetrative convection are shown on the right-hand side. Erosion of the CO_2 gradient increases CO_2 concentrations in surface waters and could maintain the water-air CO_2 gradient that drives the CO_2 efflux even in cases when atmospheric concentrations are elevated at night. Note that an increase in dissolved CO_2 concentration is not required for the entire surface mixing layer; even if small packets or eddies of water from the depth (indicated by the lower dashed line in Figure 10) are brought to the surface via plumes induced by convective mixing, their CO_2 concentration is expected to be well above the atmospheric concentration and therefore could lead to a consistent CO_2 efflux. This corresponds to the observations during the first night at Soppensee.

[45] If convective mixing is restricted to the upper layers with evenly distributed dissolved carbon dioxide (left-hand side of Figure 10), then the CO_2 concentration in the surface water is expected to be lower than during penetrative convection. The atmospheric CO_2 concentrations increase by several tens of ppmv during the evening (Figure 8d). The

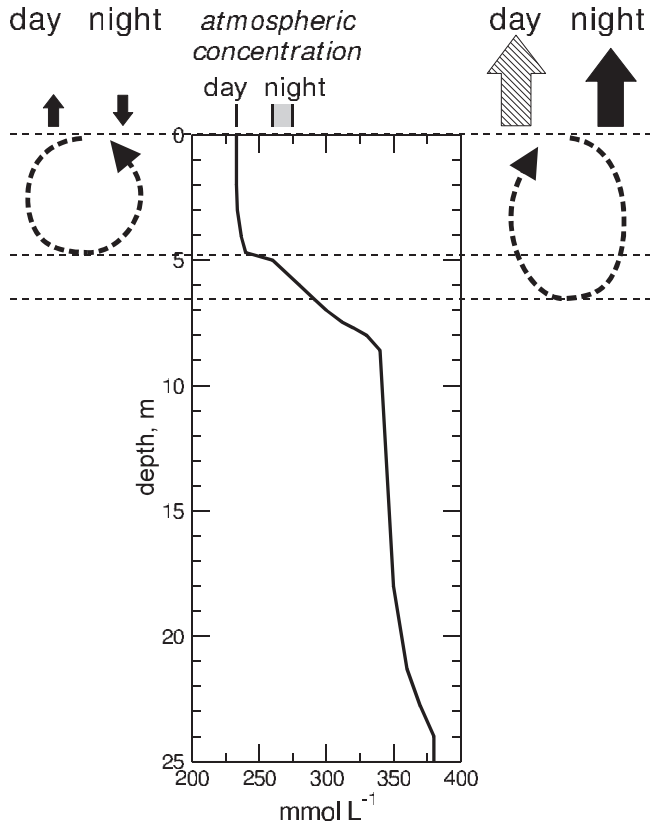

Figure 10. Schematics of the influence of convective mixing of the water column at Soppensee. The center panel shows the typical mean DIC profile for late September (data taken from spatiotemporal interpolation of measured profiles from the years 1980–1993 as presented by *Gruber et al.* [2000]). Typical atmospheric concentrations (converted using an Ostwald solubility coefficient of 0.069) during day and night are shown on top. Left: if convective mixing of the water column is nonpenetrative, then the CO_2 concentration gradient across the interface drives a flux to the atmosphere during daytime and a small flux to the lake at night. Right: if convective mixing of the water column erodes the lower epilimnion/upper hypolimnion with increased DIC concentrations, then this source of CO_2 enlarges daytime fluxes and reverses nighttime fluxes. Penetrative convection during daytime was not observed in this study. Thus the associated CO_2 efflux (shaded arrow) is hypothetical.

Table 1. Daily Net CO_2 Exchange at Soppensee (in 1998) and Toolik Lake (in 1995) as Measured With the Eddy Covariance Method and the Floating Chamber Method and Determined by Model Calculations[a]

	Soppensee		Toolik Lake	
Net CO_2 Flux	N	CO_2 Flux	N	CO_2 Flux
A: stratified periods	33	240 ± 82	59	51 ± 42
B: convective periods	54	319 ± 242	105	150 ± 45
Bx: very convective periods[b]	35	1117 ± 236	–	–
A + B: total net flux	87	289 ± 153	164	114 ± 33
Floating chamber[c]	–	–	8	365 ± 61
Concurrent EC flux[d]	–	–	16	150 ± 78
Boundary layer model[e]	–	–	602	131 ± 2
Surface renewal model[f]	–	–	597	153 ± 3
Model calculation[g]	–	164	–	–

[a]CO_2 flux values are given in mg C m^{-2} d^{-1} (mean ± standard error). N denotes number of 30-min averages in this case.
[b]Excludes the period DOY 265.95–266.42.
[c]Average of eight 1-hour chamber deployments.
[d]Average of sixteen 30-min EC flux averages matching the times of floating chamber deployments.
[e]Boundary layer model [*Cole and Caraco*, 1998] computed at 6-min resolution for the full period.
[f]Computed as done by *MacIntyre et al.* [2002] at 6-min resolution for the full period.
[g]Annual mean [*Gruber et al.*, 2000].

combination of enhanced atmospheric concentration with little or no change in the water concentration could drive an air-water concentration difference that drives a net uptake of CO_2, which could explain the observed downward CO_2 flux on DOY 266. Although there is a weak positive relationship between CO_2 gradient measurements below EC height and EC fluxes, the accuracy of our gradient measurements was not sufficient to find significant correlations. 78% of our CO_2 gradient measurements were within an estimated experimental uncertainty of ±0.8 ppm m^{-1}.

[46] Convection in lakes occurs when heat losses exceed heat inputs ($G < 0$). The transition from $G > 0$ to $G < 0$ occurs in late afternoon and persists until next morning (Figure 8d). The largest fluxes of CO_2 occurred at those times, but the strongest effluxes of CO_2 from the lake were observed during the first night of the experiment where penetrative convection occurred. A statistical unpaired two-sample *t*-test with unequal variances indicates that the mean flux of CO_2 during A and B periods does not differ significantly ($p = 0.76$). The similarity occurs because both upward and downward fluxes occurred during B periods, because mixed layer deepening did not always occur. When A periods are compared with B periods with penetrative convection (Bx in Table 1), differences in CO_2 fluxes are highly significant ($p < 0.002$).

5. Toolik Lake CO_2 Exchange

[47] Gas exchange at Toolik Lake is likely to be more complicated than at Soppensee because wind speeds were higher, and heat losses also occurred through much of the experiment and were likely to have contributed to fluxes (Figures 11c and 11d). The calculated heat fluxes (Figure 11c) indicate that the upper water column was likely to be stable only at mid-day on days 208 and 209. At other times, heat losses occurred. These were largest from late afternoon on day 208 until mid-morning on day 209 and for a similar period the following day. Heating of the upper water column occurred only during a brief period on days 210 and 211. At mid-day on 211, the upper water column frequently shifted between heat losses and heat gains. Heat losses from late afternoon to mid-morning were 4 times lower on days 211 and 212 than during days 209 and 210. On the basis of these data, penetrative convection was more likely on day 209 and 210 than on 211 and 212.

[48] The increasing CO_2 fluxes (Figure 11a) on DOY 209 section B suggests a correlation between efflux strength and the convective mixing in the lake similar to the Soppensee data. This efflux occurred even though the nocturnal CO_2 concentrations in air were well above the daytime concentrations (Figure 11b). However, because of the lack of temperature profiler data, it is not possible to relate the growth of the convective mixing layer to the efflux pattern observed in the EC flux data.

[49] During B periods on day 211, heat fluxes out of the lake are low as are the measured gas effluxes. In contrast, gas fluxes are high early on day 212 when heat loss from the lake was similarly low. This indicates that strong heat loss causing penetrative convection at the lake surface is not required for a large gas efflux. Hence the Soppensee model of Figure 10 does not necessarily also apply to arctic lakes in which CO_2 concentrations in water exceed those in the atmosphere even at night.

[50] Downward CO_2 fluxes were observed from EC measurements during A periods on day 209, 210, and 211. Surface heating ($G > 0$) occurred slightly before each of these flux events, and likely would have stratified the upper water column. A transition to heat loss from the lake occurred just prior to and during these downward fluxes (Figure 11c), and would have created a shallow mixing zone in which the turbulence created could be used to support CO_2 fluxes into the lake. However, measured CO_2 concentrations in the lake were always higher than atmospheric concentrations, and thus these downward fluxes are anomalous with respect to the observed CO_2 gradient. One possible explanation is that a downward CO_2 flux occurred at measurement height, but did not reach the lake. Because this is only likely during extremely stable atmospheric conditions, we examined the Monin-Obukhov stability parameter z/L in the atmosphere and found that during each period of downward CO_2 flux, and only during those periods, z/L was positive which indicates a more stable atmosphere (data not shown). At all other times z/L was negative and indicated good mixing conditions in the atmosphere.

[51] The CO_2 fluxes during A periods were statistically lower than during B periods at the $p < 0.06$ level. Both the boundary layer model and the surface renewal model show fluxes out of the lake during the entire period and do not show the large fluxes that occurred on day 209 and day 212. However, average fluxes obtained from these calculations and the EC measurements are similar (131 ± 2, 153 ± 3, and 114 ± 33 mg C m^{-2} d^{-1} for BLM, SRM, and EC, respectively). Chamber measurements were higher than EC, BLM, and SRM approaches during the heating period on day 208, but were similar to BLM and SRM calculations at all other times.

[52] Figure 12 shows the dependency of CO_2 fluxes as a function of the air-water temperature difference ΔT ($r^2 = 0.387$, $p < 0.001$) with a slope of −57 to −84 mg C m^{-2}

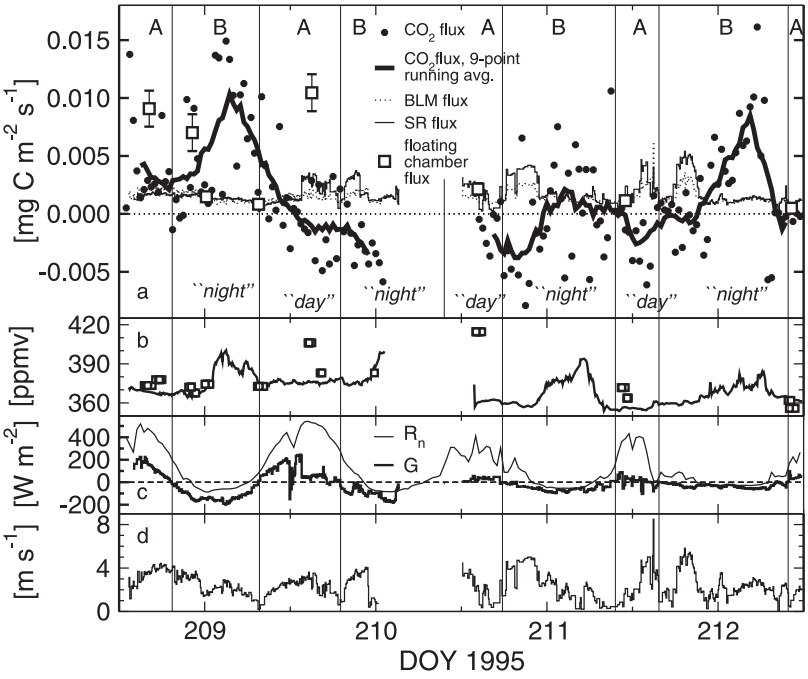

Figure 11. CO_2 fluxes (reported in carbon flux units) observed over Toolik Lake: (a) eddy covariance CO_2 flux measurements (open circles: 30-min averages; bold line: 9-point running average), boundary layer model fluxes calculated with the *Cole and Caraco* [1998] model (dashed line), and floating chamber fluxes (squares; with standard error bars); (b) atmospheric CO_2 concentrations (solid line: from eddy covariance system; squares: syringe samples analyzed in gas chromatograph); (c) net radiation (thin line) and heat exchange G across air-water interface (bold line); and (d) horizontal wind speed. The data in Figures 11b–11d are 6-min averages. Letters A and B denote stable ($G > 0$) and convective ($G \leq 0$) conditions in the epilimnion, respectively. Time is recorded as ADT and the daily solar maximum and minimum occur at 14 and 2 hours ADT, respectively.

d^{-1} K^{-1} (95% confidence interval) and an intercept between -39 and $+70$ mg C m^{-2} d^{-1}. This relationship is not expected to be universal since it implicitly also represents the difference in CO_2 concentration across the air-water interface. However, it indicates a possible relevance of convective mixing of the epilimnion for CO_2 fluxes over lakes if ΔT is an indicator of the rate of mixing in the epilimnion.

[53] The 1994 flux measurements (Figure 13) confirm the importance of convective mixing for CO_2 efflux with a clear anti-correlation between CO_2 flux and the air-water temperature difference.

6. Discussion

[54] Over ocean surfaces, there is a high degree of horizontal homogeneity of surface roughness and hence of the mechanically-induced turbulent flow field. In contrast, most lakes are well embedded within a terrestrial environment, with which they are strongly interacting [e.g., *Kocsis et al.*, 1999; *Schladow et al.*, 2002]; and the atmospheric conditions near the lake's surface are only partially determined by the exchange processes that occur over the lake itself. From the standpoint of regional and local meteorology, the fractional cover of the lakes examined in this paper is small compared to the terrestrial surface surrounding them. Therefore atmospheric conditions are largely determined by the land-surface processes, onto which the lake-surface processes superimpose a local anomaly. For example, during daytime a lake may be a cold spot in the landscape, whereas it is a hot spot at night [see also *Sun et al.*, 1998]. However, the cold lake surface during daytime

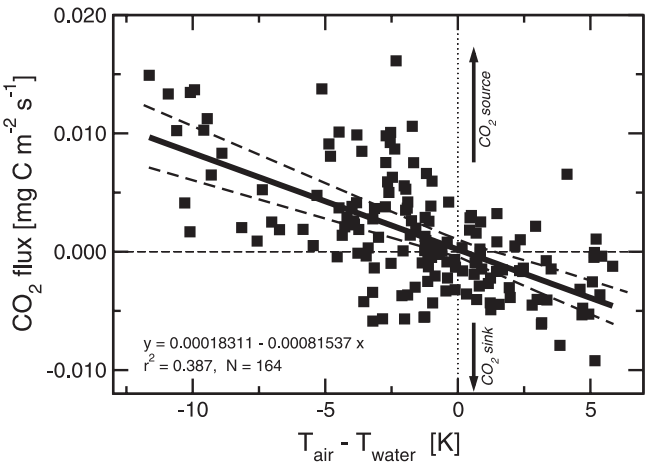

Figure 12. Correlation between the CO_2 flux over Toolik Lake and the temperature difference across the air-water interface as measured between 0.39 m above and 0.005 m below the lake surface. The solid line is the linear best fit, and the dashed lines indicate the 95% confidence interval of the fit.

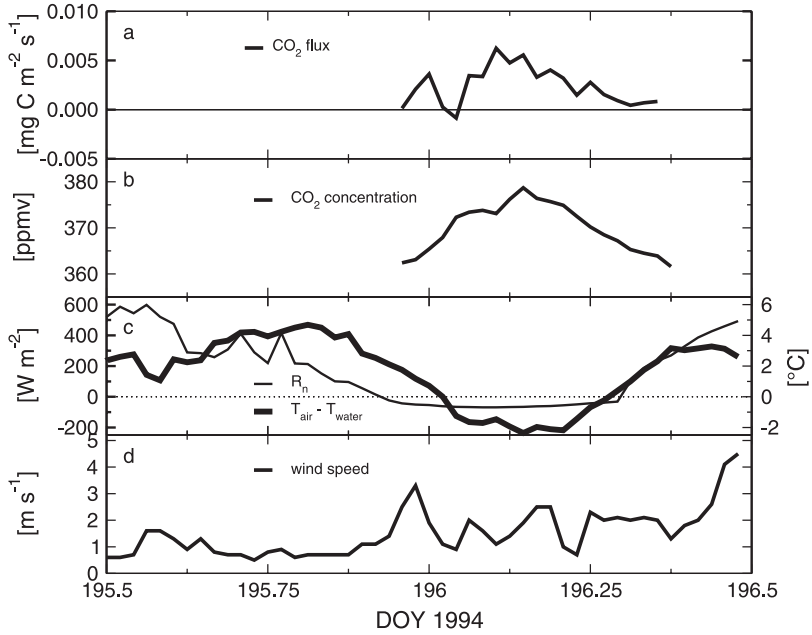

Figure 13. Eddy covariance flux measurements during the 1994 Toolik Lake experiment. (a) CO_2 flux; (b) atmospheric CO_2 concentration; (c) net radiation (thin line) and temperature difference measured between 1.5 m above and 0.05 m below the lake surface (thick line); (d) horizontal wind speed. Averaging time is 30 min.

does not necessarily imply that the atmosphere above it is stably stratified; turbulent eddies nourished by the heat flux from a nearby warm land surface are large enough to impose turbulent and unstable conditions over the cold lake surface. At Toolik Lake, for instance, the atmospheric surface layer was unstable ($z/L < 0$) during 71% of the time while ΔT across the air-water interface was negative only during 66% of the time (during the Soppensee experiment z/L indicated unstable atmospheric conditions at all times). At night, heat exchange across the warm surface keeps the near-surface layer above the lake unstably stratified, but cold, potentially moist and CO_2-rich air is advected from the upwind lake shore onto the surface, leading to potentially rapid increases in atmospheric CO_2 concentrations at night. These are not a result of local outgassing of CO_2 from the lake, but could significantly modify the flux across the air-water interface via the change in CO_2 gradient. This is in contrast to open ocean conditions where the atmospheric concentration is assumed constant.

[55] Another important difference between CO_2 fluxes over oceans and over lakes is related to the proximity of CO_2 sources. The ultimate source of CO_2 may be linked to organic matter in the sediments or the influx of CO_2-rich groundwater into the lake, and all but the largest and deepest lakes are closer to these sources than are the oceans. In addition, regardless of the ultimate source of CO_2, the proximate source is most often related to the patterns of vertical stratification in the lake. The differences in CO_2 concentrations between surface and metalimnetic or bottom waters are usually higher in lakes than in oceans, and the physical separation between such low versus high zones of CO_2 is lower in lakes than oceans (i.e., thermocline depths are shallower in lakes). Given these general differences in physical and chemical characteristics, a given input of mixing energy will more often tap into sources of CO_2-rich water in a lake than in an ocean. The measurements from Soppensee illustrate how important penetrative convection is, especially in regards to the striking difference between the CO_2 efflux observed early on DOY 265 versus the CO_2 flux in the opposite direction early on DOY 266. In addition to the correlations of convective mixing and increased CO_2 flux, evidence of a physical mechanism is provided for by the pattern of surface currents observed with the ADCP in Soppensee. The patterns indicate strong downward plumes with a characteristic core diameter on the order of 5 m [*Jonas et al.*, 2003] during the night. During the day, vertical velocities were typically below 1 mm s^{-1} and did not exhibit much structure [*Jonas et al.*, 2003].

[56] The great variability of EC CO_2 fluxes, especially during periods with convective mixing of the epilimnion, is consistent with the operation of such plume structures in a chemically stratified water body. Footprint estimates of the EC flux measurements were performed using the *Schmid* [1997] source area model. The footprint is defined as the surface area upwind from the EC instruments that directly influences the magnitude of the observed fluxes. If the footprint is completely over the lake surface, then advective influences from the land do not significantly contaminate the EC measurements. However, if the footprint includes a relevant proportion of the land, then the EC flux measurements are no longer representative for the lake surface alone. On Soppensee the characteristic dimensions of the surface area that contributes 90% to the total flux measurement under unstable conditions was as follows: The instruments do not "see" the surface closer than 15 m from the mast; the point of maximum contribution is roughly 45 m upwind; the far end of the 90% isoline is at 120 m upwind (thus still within the nearest distance to the shore which was

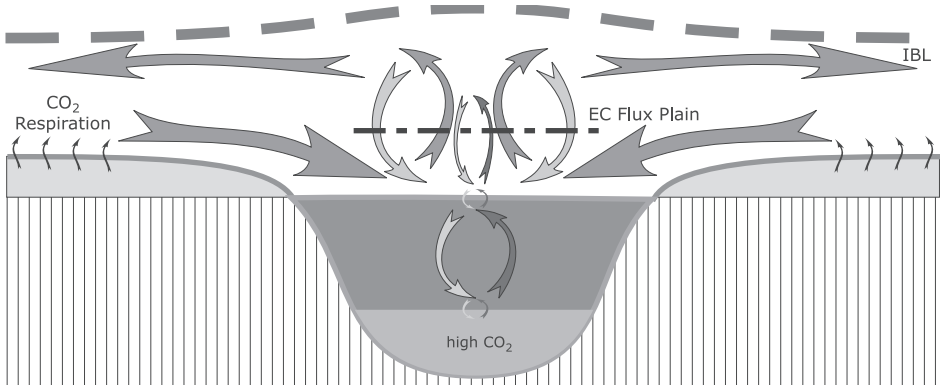

Figure 14. Processes influencing the eddy covariance (EC) flux measurements above a lake surface at night. Because EC measurements cannot be performed directly at the air-water interface, the CO_2 exchange with the lake (blue and red arrows) at EC reference height (black dash-dotted line) is measured together with the exchange flux of CO_2-rich air from the land surrounding the lake (pink and yellow arrows) where CO_2 originates from respiration of soils and vegetation (black arrows). This local lake-breeze type circulation is expected to be restricted in its vertical extent by an internal boundary layer (IBL). See color version of this figure at back of this issue.

125–440 m away); and the maximum width of the footprint is 16 m (values computed for $z = 2.8$ m, $z_0 = 0.001$ m, $z/L = -0.2$, and $\sigma_v/u_* = 1.5$; the z_0 and σ_v/u_* estimates were derived from our measurements). These values indicate that the flux measurements from Soppensee during convective periods (where both the epilimnion and the atmospheric surface layer are convective) integrate over a lake surface area that contains a few plumes only. Therefore we hypothesize that some of the observed EC flux variability could be caused by significant differences in the plume-related vertical CO_2 fluxes in the epilimnion. In this case we would expected that the atmospheric turbulence and stability as well as the diurnal cycle of CO_2 concentrations in air are the most relevant factors governing the physics of gas exchange at the water surface, in addition to the availability of these variable and intermittent sources of CO_2. The 90% footprint area at Toolik Lake for similar conditions extended between 6 and 52 m upwind with a maximum contribution from roughly 20 m upwind. With increasing stability the footprints in both cases grow larger than the values given here.

[57] Footprint modeling is however still a controversial issue. Although the *Schmid* [1997] model yields similar values for the point of maximum contribution as the *Schuepp et al.* [1990] model, the assumptions for the trailing end of the footprint and thus for the potential contribution of the land surface to fluxes measured over the lake are not identical. *Schmid* [2002] provides a thorough review of various footprint calculations and addresses their limitations and weaknesses. Figure 14 illustrates the problem for CO_2 flux measurements over small lakes during nocturnal conditions where the lake is warmer than the surrounding land surface and wind speeds are near calm. Within an internal boundary layer (IBL) a local circulation between the land and lake is expected to transport CO_2 originating from terrestrial ecosystem respiration to the lake [see *Sun et al.*, 1998, 2001]. At the same time, CO_2 is mixed above the lake surface, is exchanged between atmosphere and the lake, and is mixed in the lake by convection, potentially eroding CO_2-rich waters at depth when convection is penetrative. Since EC measurements are not made at the surface but at some height above it, the flux from the lake surface must be separated from the advective flux from the land/lake interaction. Our approach was to use shorter averaging times for covariances at Soppensee which acts as a high-pass filter that is supposed to eliminate contributions from larger eddies that are most likely associated with the exchange between land and lake. At the same time, it is obvious that by reducing the averaging time we also miss some low-frequency contributions that are not related to exchange processes between land and lake. In future studies we suggest to measure even closer to the surface than we did, provided that the IRGA has a shorter optical path length and is capable of at least 20 Hz temporal resolution. This should increase the confidence that the EC flux is not significantly influenced by land/lake interactions. The trade-off is the larger loss on the high-frequency end of the flux cospectra. The gain at the low-frequency end of the cospectra appears to be beneficial despite the increase in high-frequency losses.

[58] Biological processes were not treated explicitly in this study. It should therefore be kept in mind that photosynthesis during daytime and respiration during nighttime also influence the CO_2 concentrations in surface waters, thereby acting as a local sink during the day and a source during the night. However, the great variability in CO_2 flux that is only observed during convective (nocturnal) periods but not during daytime strongly indicates that biological processes alone cannot explain the observed differences in gas fluxes between convective and nonconvective conditions.

[59] Profiles of dissolved CO_2 concentrations in Toolik Lake are unavailable for the 1995 campaign, but typical profiles in July show surface values of $\approx$20–30 μM CO_2 and values at the base of the metalimnion ($\approx$8 m depth) of 50–60 μM. Such differences indicate the potential for penetrative convection to tap into CO_2-rich water and bring it to the surface, thus enhancing both the variability and magnitude of CO_2 flux to the atmosphere. Although mixing to 8 m depth was improbable during our study period, later in the season when heat losses are greater, even higher effluxes are likely.

[60] The flux footprint areas were smaller over Toolik Lake than over Soppensee because of the lower instrument height. The small footprint may have contributed to the high variability of 30-min flux averages. The chamber measurements and BLM and SRM models always indicated a net efflux out of the lake, whereas the EC measurements sometimes indicated fluxes into the lake. While the bulk measurements of CO_2 concentrations in the lake indicate that fluxes should be outward, if surface waters were stably stratified, biological activity could draw down CO_2 concentrations and lead to lower values in a thin layer near the air-water interface [*Soloviev et al.*, 2001]. While the chambers always measured an efflux integrated over their full deployment ($\approx$60 min), during two partial periods of measurement within two different deployments the CO_2 concentration in the chamber decreased, indicating an uptake of CO_2 by the lake. These periods of measurement occurred during the A period in the afternoon of DOY 210 and at the very end of the measurements made on DOY 212. At these two times the EC flux was also into the lake, and G was positive, indicating surface heating and the probable creation of a shallow mixed layer. CO_2 drawdown in this layer, calculated on the basis of average photosynthetic rates in surface waters at Toolik in late July (24 mg C m^{-3} d^{-1}), was insufficient to change the sign of the CO_2 gradient and account for the downward flux.

[61] Downward fluxes were also measured at other times by EC and corresponded to periods of heat losses during the day. At those times, the surface renewal model calculated a high gas transfer velocity due to the energy from wind and heat loss being trapped in a shallow mixed layer. At these times the mixing layers were likely large enough that the measured concentrations of CO_2 were accurate and effluxes would have been out of the lake. Two explanations for the apparent counter-gradient fluxes are likely. First, our data indicate that these anomalous downward EC fluxes of CO_2 only occurred during relatively stable atmospheric conditions when the confounding influence of CO_2 advection from land may be strongest. Alternatively, because the measured fluxes were low the absolute accuracy of the EC flux measurements could have been reached. In either case, it is apparent that under such conditions higher-quality EC flux instruments are needed to increase confidence in the measurements. Therefore our Toolik Lake data recorded under such conditions may be less reliable than chamber or model results.

[62] Chamber estimates of fluxes were higher than those calculated by the SRM and BLM. These two calculation procedures provided similar average fluxes over the measurement period compared to EC. The surface renewal model has been used primarily in laboratory studies and in a few oceanographic studies (reviewed by *MacIntyre et al.* [1995], *Soloviev and Schluessel* [1994, 2001], *Soloviev et al.* [2001]). It was applied here using estimated mixed layer depths, but it does provide similar long term averages to the BLM. Calculated fluxes were higher with this model than the BLM during periods of heat loss and during periods when the actively mixing layer was shallow. Similarly, *Soloviev and Schluessel* [2001] found gas transfer velocities to be higher when heat loss and bubble production are taken into account. Soloviev and Schluessel's model does not take into account penetration of short wave irradiance into the mixing layers and below, and hence will underestimate fluxes. Gas transfer velocities calculated with the surface renewal model supported the EC measurements in the Soppensee, indicating that fluxes were stronger when mixing due to convection occurred and fluxes would be damped with surface heating. With further development, the surface renewal model may provide a critical need of more accurate estimates of gas flux over sheltered water bodies where winds are low and estimates of gas flux using wind-based boundary layer models are not likely to be accurate.

7. Conclusions

[63] Direct CO_2 exchange measurements above two lake surfaces apparently show the importance of convective mixing in surface waters for the CO_2 flux. The temporal pattern of CO_2 fluxes is more complex than initially expected, making it difficult to use simple wind-speed based empirical relationships to gain a predictive understanding of the CO_2 flux. Significant differences between the governing physical exchange processes over lakes and the oceans may exist with respect to the horizontal homogeneity of the water and air surfaces, as well as the proximity to local sources of CO_2-rich water. This study clearly demonstrates that the EC method can provide the necessary temporal resolution and coverage to resolve the importance of relevant processes like penetrative convection, which were neglected in earlier estimates and measurements of CO_2 effluxes from lakes.

[64] There were strong and significant differences between CO_2 fluxes observed during nonconvective and convective conditions within the lakes. The Soppensee data revealed that CO_2 fluxes are increased by a factor 4.7 during periods with penetrative convection compared to stably stratified periods. Not only does penetrative convection increase gas fluxes during periods with low wind, the associated entrainment of metalimnetic water may lead to increased gas concentrations in surface waters and appreciably enhance gas flux. Thus the process of penetrative convection is most important to gas fluxes when it is coupled to vertical stratification of CO_2 in the water.

[65] The Soppensee measurements indicate close agreement between the surface energy budget derived from the EC method, the temperature profiler approach, and the calorimetric heat budget computed from a thermistor chain. The Soppensee results indicate that careful selection of high-quality EC instrumentation in combination with vertical profile information from the water body are most promising for future research. CO_2 exchange across lake surfaces is a three-dimensional phenomenon and has links to its terrestrial surroundings. Therefore one-dimensional approaches that are well suited for application over ocean surfaces may not succeed under the circumstances typically found for inland waters. While boundary layer models and chamber measurements may result in similar estimates of CO_2 flux compared to EC results, the former methods are incapable of clarifying the important physical mechanisms controlling gas flux. The surface renewal model, however, holds more promise for illustrating operative physical processes. Explicit consideration of the convective conditions in lakes could lead to significantly larger estimates of CO_2 efflux, depending on the frequency of their occurrence

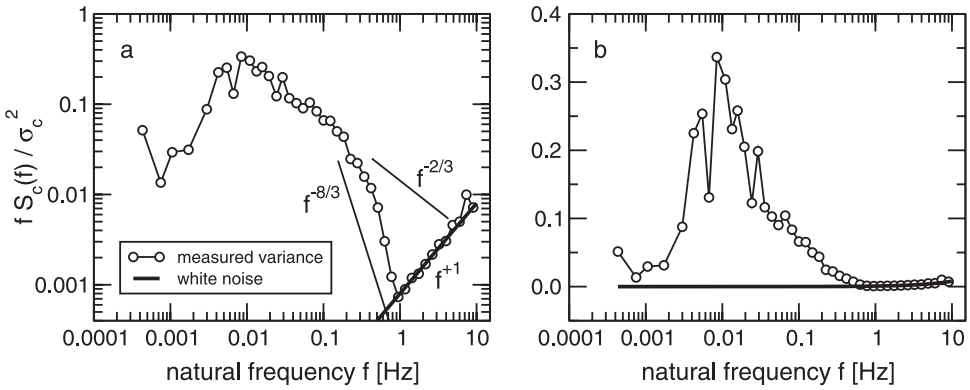

Figure 15. Determination of noise level and signal-to-noise ratio (SNR) from measured data. Figures 15a and 15b are the same display of an example variance spectrum of CO_2 concentration measured with a LiCOR 6252 IRGA at Toolik Lake (1-s internal averaging, oversampled at 20 Hz). Figure 15a displays the measured curve (thin line with open symbols) and fitted white noise level (bold line) in a fashion where the frequency-independent noise level becomes a straight line with slope f^{+1}. The theoretical slopes of the inertial subrange are also given for undamped ($\propto f^{-2/3}$) and damped ($\propto f^{-8/3}$) spectra. Figure 15b provides an equal-area view of the same curves. See text for further details.

in a given environment. For instance, gas transfer velocities calculated using the surface renewal model for tropical lakes suggest that fluxes are likely to be underestimated there by a factor of at least 2 [*MacIntyre et al.*, 2001] and our study indicates that fluxes based on wind based models may be low by 150%. Therefore future studies in water bodies from the tropics to the Arctic should include these measurement approaches that elucidate the times when fluxes occur and models that can accurately represent them.

Appendix A: Noise Levels and Measurement Accuracy

A1. Noise in the LiCOR 6252

[66] A LiCOR 6252 infrared gas analyzer was used at Toolik Lake. To investigate its noise level we define the RMS noise as the error when measuring the same quantity multiple times, without including systematic errors due to uncertainty in estimating the calibration constants. The LiCOR 6252 provides data with 1-second temporal resolution which we oversampled at 20 Hz with our set-up. Thus all information in the frequency range >1 Hz is noise without signal and can be used to determine the true noise level during operation in the field.

[67] Figure 15a indicates how this is done. Since the spectral density of the CO_2 variance is multiplied by frequency in this representation, random noise is found by fitting a straight line with slope 1 (the "white noise" line) to the data >1 Hz (note that random noise is independent of frequency and averaging time, hence the f^{+1} behavior, where f is the natural frequency in Hz). Figure 15b shows the same graph, but with a linear y-axis, which provides an equal-area representation of each proportion under the displayed curve [cf. *Stull*, 1988, p. 315]. This kind of display gives the correct visual proportions between the variances of the signal and the noise. To achieve this equal-area display, the spectral densities must be multiplied by f, since $d\ln|f| = df/f$ on the x-axis. Finally, the RMS noise is the square-root of the variance determined by that fitted line.

[68] Figure 16 shows the time evolution of the RMS noise determined in this manner from our LiCOR 6252 data from Toolik Lake. The mean RMS noise level was found to be 0.022 ppm (line A). The noise level reported by *Donelan and Drennan* [1995] for a LiCOR 6262 operated at full 10-Hz temporal resolution is indicated by line B. By increasing the internal averaging time of the LiCOR 6262 from 0.1 to 1 s would lower the noise level by a factor $\sqrt{1/0.1} = 3.2$, which closely corresponds with the ratio between lines A and B in Figure 16.

A2. Signal-to-Noise Ratio

[69] The signal-to-noise ratio (SNR) is defined as [e.g., *Donelan and Drennan*, 1995]

$$\mathrm{SNR} = \sqrt{\frac{\overline{c'^2}}{(\mathrm{RMS\ noise})^2} - 1}. \qquad \text{(A1)}$$

The SNR is a function of frequency since RMS noise is independent of frequency while the signal shows a

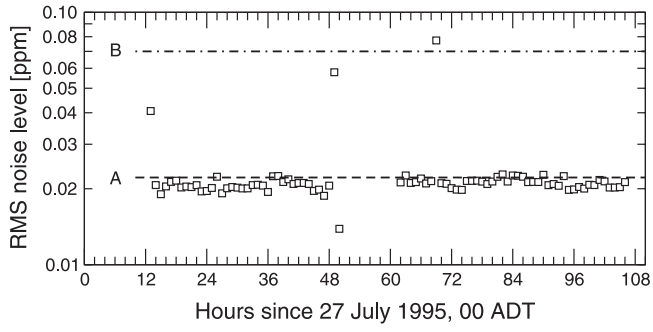

Figure 16. RMS noise levels of the LiCOR 6252 IRGA with 1-s output resolution automatically determined from variance spectra for each 30-min interval (squares), the overall mean (line A), and the mean reported by *Donelan and Drennan* [1995] for a 10-Hz resolving instrument (line B). The ratio of B/A closely corresponds with the expected theoretical ratio of 3.2 (see text).

characteristic frequency spectrum. Equation (A1) can therefore be clarified by writing

$$\mathrm{SNR}(f) = \sqrt{\frac{\overline{c(f)'^2}}{(\mathrm{RMS\ noise})^2} - 1} \qquad \text{(A2)}$$

for the SNR observed at a specific frequency.

[70] In Figure 15, for example, the SNR($f > 1$ Hz) = 0, since the LiCOR 6252 has an output resolution of 1 Hz. For eddy covariance flux measurements, however, a low SNR at high frequency is not a concern, since the SNR tends to get very large toward the low frequencies. When averaging over 5 or 30 min (or even longer periods), the signal used for the variance and covariance computations is taken from all frequencies above the truncation frequency determined by the length of the averaging period. Thus, in this paper, we report the SNR as the average of $f > 0.0033$ Hz, which is the truncation frequency of a 5-min averaging period.

A3. Accuracy of Flux Measurements

[71] The covariance $\overline{w'c'}$ is related to the variances of the vertical wind speed σ_w^2 and of the CO_2 fluctuations σ_c^2 via the correlation coefficient $r_{w,c}$ [e.g., *Wilks*, 1995, p. 46],

$$r_{w,c} = \frac{\overline{w'c'}}{\sigma_w \cdot \sigma_c}. \qquad \text{(A3)}$$

[72] Under the assumption that noise is random, and that noise in w is not correlated with noise observed in c (that is, $r_{w,c} = 0$), then the covariance should be zero no matter how high the noise level in either signal is. In reality, this is not perfectly the case, and thus we performed an experiment by putting our sonic anemometer sensor head together with the NOAA IRGA into a cardboard box that was coated with plastic bubble wrap to minimize acoustic reflections inside the box. The box was then loosely sealed with tape in order to allow for heat and CO_2 exchange with the laboratory.

[73] Data were collected at 20 Hz sampling rate during 20 hours and then processed as 30-min and 5-min averages. The last 9 hours (nighttime, undisturbed) were used to estimate the minimum repeatable CO_2 flux measurement, and the first 7 hours (daytime, with disturbances) were used to analyze the potential effects of quick changes in CO_2 concentration inside the box on the computed covariances.

A3.1. Minimum Repeatable CO_2 Flux Measurement

[74] The CO_2 concentration in the box was 461 ppm (laboratory background concentration), dropping from 477 ppm after the last person had left to 448 ppm before the first person arrived the next morning. The root-mean-square standard deviation of the CO_2 flux measurements were between 0.197 and 0.292 ppm with an average of 0.219 ppm for the 5-min averaging interval, and 0.202–0.800 ppm (average 0.443 ppm) for the 30-min averaging interval, thus indicating that the trend in concentration has a larger influence with the longer averaging time. Nevertheless, the arbitrary CO_2 fluxes ranged between $-1.26 \cdot 10^{-4}$ and $4.6 \cdot 10^{-5}$ mg C m^{-2} s^{-1}, and between $-3.9 \cdot 10^{-5}$ and $2.2 \cdot 10^{-5}$ mg C m^{-2} s^{-1} when averaged over 5 and 30 min intervals, respectively. This is at least two orders of magnitude better than what would be needed to resolve the fluxes reported in our paper. Thus, despite the clearly higher noise level of the NOAA IRGA used at Soppensee, the accuracy of the flux measurements does not seem to be seriously affected by noise. However, the large density flux corrections according to *Webb et al.* [1980] remain a concern for accurate EC flux measurements over water surfaces.

[75] The RMS standard deviations of the wind vector components were largest for the vertical component. Our measurements were between 0.008 and 0.015 m s^{-1}, and the correlation coefficient between the noise in c and the one in w (equation (A3)) was between -0.111 and 0.052 for the 5-min averaging intervals. When averaging was done over 30 min, all variances and correlations got closer to zero roughly by the same factor as the length of the averaging period increased. If noise in w and c were of the same source and thus $r_{w,c} = 1$, the apparent flux computed with equation (A3) would still only be 0.002 mg C m^{-2} s^{-1} at worst.

[76] Our minimum repeatable CO_2 flux measurement derived in this laboratory experiment under controlled and undisturbed conditions was better than $1.3 \cdot 10^{-4}$ and $3.9 \cdot 10^{-5}$ mg C m^{-2} s^{-1} for 5 and 30 min averaging times, respectively.

A3.2. Effect of Disturbance on the CO_2 Flux Measurement

[77] To simulate the effect of advection of high concentrations of CO_2 from the land to the lake we allowed people access to the laboratory where we carried out our zero flux experiment. The CO_2 concentration thus varied between 450 and 560 ppm during the first 7 hours of the experiment. The steepest increase observed was 102 ppm within 30 min. The largest (absolute magnitude) of apparent CO_2 flux measured inside our box was 0.001 and 0.005 mg C m^{-2} s^{-1} for the 5 and 30 min averages, respectively. Although the change in CO_2 concentration in this simulation was much larger than what was observed over Soppensee, the apparent fluxes are at least one order of magnitude smaller than the peaks in our measurements during convective conditions. Moreover, this experiment clearly demonstrates the expected effect that 5-min averages are less sensitive to such erratic occurrences (or advection) than 30-min averages.

[78] This is not to say that advection is not a relevant issue. It is to be interpreted in the way that advection is a relevant source for the high CO_2 concentration over our lakes observed at night, but the eddy covariance method, since it is a method to measure turbulent, not advective fluxes, is quite robust against such effects.

[79] **Acknowledgments.** The Toolik Lake measurements were performed as a part of the Arctic System Science Flux Study funded by U.S. National Science Foundation grants OPP-9318532 (F.S.C.), 9318529, and 9615949 (G.K.). Measurements at Soppensee were funded by the Swiss National Science Foundation, grants 20-50761.97 and 2000-063723.00. W.E. was funded by a Hans Sigrist Fellowship grant of the University of Bern for analyzing the data and publishing the results. S.M. was supported by NSF grants DEB9726930 and DEB0108572. We thank William S. Reeburgh for the loan of the LI-COR 6252 instrument during the 1995 experiment and Rolf Siegwolf and Peter Geissbühler, PSI, for the loan of a LI-COR 6262 instrumental setup used for gradient measurements at Soppensee. Gilda Gamarra, Ian Moore, Bryan Harper, Tom Ravens, and Michael Schurter provided support in the field. Lorenz Moosmann assisted

with data analysis. William Drennan, University of Miami, kindly helped to clarify the issue on signal-to-noise ratios, and three anonymous reviewers helped to improve the manuscript.

References

Anderson, D. E., R. G. Striegl, D. I. Stannard, C. M. Michmerhuizen, T. A. McConnaughey, and J. W. LaBaugh, Estimating lake-atmosphere CO_2 exchange, *Limnol. Oceanogr.*, *44*, 988–1001, 1999.

Arya, S. P. S., *Introduction to Micrometeorology*, 307 pp., Academic Press, San Diego, 1988.

Auble, D. L., and T. P. Meyers, An open path, fast response infrared absorption gas analyzer for H_2O and CO_2, *Boundary Layer Meteorol.*, *59*, 243–256, 1992.

Baldocchi, D., A comparative study of mass and energy exchange rates over a closed C_3 (wheat) and an open C_4 (corn) crop: II. CO_2 exchange and water use efficiency, *Agric. For. Meteorol.*, *67*, 291–321, 1994.

Belanger, T. V., and E. A. Korzun, Critique of the floating-dome technique for estimating reaeration rates, *J. Environ. Eng.*, *117*, 144–150, 1990.

Cole, J. J., and N. F. Caraco, Atmospheric exchange of carbon dioxide in a low-wind oligotrophic lake measured by the addition of SF_6, *Limnol. Oceanogr.*, *43*, 647–656, 1998.

Cole, J. J., N. F. Caraco, G. W. Kling, and T. K. Kratz, Carbon dioxide supersaturation in the surface waters of lakes, *Science*, *265*, 1568–1570, 1994.

Crill, P., K. B. Bartlett, J. D. Wilson, D. K. Sebacker, R. C. Harriss, J. M. Melack, S. MacIntyre, L. Lesack, and L. Smith-Morrill, Trophospheric methane from an Amazon floodplain lake, *J. Geophys. Res.*, *93*, 1564–1570, 1988.

Deardorff, J. W., Convective velocity and temperature scales for unstable planetary boundary layer and for Rayleigh convection, *J. Atmos. Sci.*, *27*, 1211–1213, 1970.

Donelan, M. A., and W. M. Drennan, Direct field measurements of the flux of carbon dioxide, in *Air-Water Gas Transfer*, edited by B. Jähne and E. C. Monahan, pp. 677–683, Aeon-Verlag, Heidelberg, Germany, 1995.

Edwards, G. C., H. H. Neumann, G. den Hartog, G. W. Thurtell, and G. E. Kidd, Eddy correlation measurements of methane fluxes using a tunable diode laser at the Kinosheo Lake tower site during the Northern Wetlands Study (NOWES), *J. Geophys. Res.*, *99*, 1511–1517, 1994.

Eugster, W., and W. Senn, A cospectral correction model for measurement of turbulent NO_2 flux, *Boundary Layer Meteorol.*, *74*, 321–340, 1995.

Fairall, C. W., J. E. Hare, J. B. Edson, and W. McGillis, Parameterization and micrometeorological measurement of air-sea gas transfer, *Boundary Layer Meteorol.*, *96*, 63–105, 2000.

Field, R. T., L. J. Fritschen, E. T. Kanemasu, E. A. Smith, J. B. Stewart, S. B. Verma, and W. P. Kustas, Calibration, comparison, and correction of net radiation instruments used during FIFE, *J. Geophys. Res.*, *97*, 18,681–18,695, 1992.

Francey, R. J., and J. R. Garratt, Eddy flux measurements over the ocean and related transfer coefficients, *Boundary Layer Meteorol.*, *14*, 153–166, 1978.

Fritschen, L. J., Construction and calibration details of the thermal-transducer-type net radiometer, *Bull. Am. Meteorol. Soc.*, *41*, 180–183, 1960.

Gruber, N., B. Wehrli, and A. Wüest, The role of biogeochemical cycling for the formation and preservation of varved sediments in Soppensee, *J. Paleolimnol.*, *24*, 277–291, 2000.

Horst, T. W., On frequency response corrections for eddy covariance flux measurements, *Boundary Layer Meteorol.*, *94*, 517–520, 2000.

Imberger, J., The diurnal mixed layer, *Limnol. Oceanogr.*, *30*, 737–770, 1985.

Jonas, T., A. Wüest, A. Stips, and W. Eugster, Observations of a quasi-shear-free convective boundary layer: Stratification and its implications on turbulence, *J. Geophys. Res.*, *108*, doi:10.1029/2002JC001440, in press, 2003.

Jones, E. P., and S. D. Smith, A first measurement of sea-air CO_2 flux by eddy correlation, *J. Geophys. Res.*, *82*, 5990–5992, 1977.

Kaimal, J. C., and J. J. Finnigan, *Atmospheric Boundary Layer Flows: Their Structure and Measurement*, 289 pp., Oxford Univ. Press, New York, 1994.

Kaimal, J. C., J. C. Wyngaard, Y. Izumi, and O. R. Coté, Spectral characteristics of surface-layer turbulence, *Q. J. R. Meteorol. Soc.*, *98*, 563–589, 1972.

Kling, G. W., G. W. Kipphut, and M. C. Miller, Arctic lakes and streams as gas conduits to the atmosphere: Implications for tundra carbon budgets, *Science*, *251*, 298–301, 1991.

Kling, G. W., G. W. Kipphut, and M. C. Miller, The flux of carbon dioxide and methane from lakes and rivers in arctic Alaska, *Hydrobiologia*, *240*, 23–36, 1992.

Kling, G. W., G. W. Kipphut, M. C. Miller, and W. J. O'Brien, Integration of lakes and streams in a landscape perspective: The importance of material processing on spatial patterns and temporal coherence, *Freshwater Biol.*, *43*, 477–497, 2000.

Kocsis, O., H. Prandke, A. Stips, A. Simon, and A. Wüest, Comparison of dissipation of turbulent kinetic energy determined from shear and temperature microstructure, *J. Mar. Syst.*, *21*, 67–84, 1999.

Lenschow, D. H., Micrometeorological techniques for measuring biosphere-atmosphere trace gas exchange, in *Biogenic Trace Gases: Measuring Emissions From Soil and Water*, *Methods Ecol.*, edited by P. A. Matson and R. C. Harriss, pp. 126–163, Blackwell Sci., Malden, Mass., 1995.

Leuning, R., and M. J. Judd, The relative merits of open- and closed-path analysers for measurement of eddy fluxes, *Global Change Biol.*, *2*, 241–253, 1996.

Leuning, R., and K. M. King, Comparison of eddy-covariance measurements of CO_2 flux by open- and closed-path CO_2 analysers, *Boundary Layer Meteorol.*, *59*, 297–311, 1992.

Leuning, R., and J. Moncrieff, Eddy-covariance CO_2 flux measurements using open- and closed-path CO_2 analysers: Corrections for analyser water vapour sensitivity and damping of fluctuations in air sampling tubes, *Boundary Layer Meteorol.*, *53*, 63–76, 1990.

Leuning, R., O. T. Denmead, A. R. G. Lang, and E. Ohtaki, Effects of heat and water vapor transport on eddy covariance measurement of CO_2 fluxes, *Boundary Layer Meteorol.*, *23*, 209–222, 1982.

Livingston, G. P., and G. L. Hutchinson, Enclosure-based measurement of trace gas exchange: Applications and sources of error, in *Biogenic Trace Gases: Measuring Emissions From Soil and Water*, *Methods Ecol.*, edited by P. A. Matson and R. C. Harriss, pp. 14–51, Blackwell Sci., Malden, Mass., 1995.

Lotter, A. F., Evidence of annual layering in Holocene sediments of Soppensee, Switzerland, *Aquat. Sci.*, *51*, 19–30, 1989.

MacIntyre, S., R. Wanninkhof, and J. P. Chanton, Trace gas exchange across the air-water interface in freshwater and coastal marine environments, in *Biogenic Trace Gases: Measuring Emissions From Soil and Water*, *Methods Ecol.*, edited by P. A. Matson and R. C. Harriss, pp. 52–97, Blackwell Sci., Malden, Mass., 1995.

MacIntyre, S., K. M. Flynn, R. Jellison, and J. R. Romero, Boundary mixing and nutrient fluxes in Mono Lake, California, *Limnol. Oceanogr.*, *44*, 512–529, 1999.

MacIntyre, S., W. Eugster, and G. W. Kling, The critical importance of buoyancy flux for gas flux across the air-water interface, in *Gas Transfer at Water Surfaces*, *Geophys. Monogr. Ser.*, vol. 127, edited by M. A. Donelan et al., pp. 135–139, AGU, Washington, D.C., 2001.

MacIntyre, S., J. R. Romero, and G. W. Kling, Spatial-temporal variability in mixed layer deepening and lateral advection in an embayment of Lake Victoria, East Africa, *Limnol. Oceanogr.*, *47*, 656–671, 2002.

Massman, W. J., A simple method for estimating frequency response corrections for eddy covariance systems, *Agric. For. Meteorol.*, *104*, 185–198, 2000.

Massman, W. J., and X. Lee, Eddy covariance flux corrections and uncertainties in long-term studies of carbon and energy exchanges, *Agric. For. Meteorol.*, *113*, 121–144, 2002.

Matson, P. A., and R. C. Harriss (Eds.), *Biogenic Trace Gases: Measuring Emissions from Soil and Water*, *Methods Ecol.*, 394 pp., Blackwell Sci., Malden, Mass., 1995.

McGillis, W. R., J. B. Edson, J. E. Hare, and C. W. Fairall, Direct covariance air-sea CO_2 fluxes, *J. Geophys. Res.*, *106*, 16,729–16,745, 2001.

McMillen, R. T., An eddy correlation technique with extended applicability to non-simple terrain, *Boundary Layer Meteorol.*, *43*, 231–245, 1988.

O'Brien, W. J., et al., The limnology of Toolik Lake, in *Freshwaters of Alaska: Ecological Syntheses*, *Ecol. Ser.*, vol. 119, edited by A. M. Milner and M. W. Oswood, pp. 61–106, Springer-Verlag, New York, 1997.

Ocampo-Torres, F. J., M. Donelan, N. Merzi, and F. Jia, Laboratory measurements of mass transfer of carbon dioxide and water vapour for smooth and rough flow conditions, *Tellus, Ser. B*, *46*, 16–32, 1994.

Ohmura, A., and K. Schroff, Physical characteristics of the Davos-type pyrradiometer for short- and long-wave radiation, *Arch. Meteorol. Geophys. Bioklimatol., Ser. B*, *33*, 57–76, 1983.

Panofsky, H. A., and J. A. Dutton, *Atmospheric Turbulence*, 397 pp., John Wiley, New York, 1984.

Rannik, Ü., and T. Vesala, Autoregressive filtering versus linear detrending in estimation of fluxes by the eddy covariance method, *Boundary Layer Meteorol.*, *91*, 259–280, 1999.

Richey, J. E., J. M. Melack, A. K. Aufdenkampe, V. M. Ballester, and L. L. Hess, Outgassing from Amazonian rivers and wetlands as a large tropical source of atmospheric CO_2, *Nature*, *416*, 617–620, 2002.

Schladow, S. G., M. Lee, B. E Hrzeler, and P. B. Kelly, Oxygen transfer across the air-water interface by natural convection in lakes, *Limnol. Oceanogr.*, *47*, 1394–1404, 2002.

Schmid, H. P., Experimental design for flux measurements: Matching scales of observations and fluxes, *Agric. For. Meteorol.*, *87*, 179–200, 1997.

Schmid, H. P., Footprint modeling for vegetation atmosphere exchange studies: A review and perspective, *Agric. For. Meteorol.*, *113*, 159–183, 2002.

Schuepp, P. H., M. Y. Leclerc, J. I. MacPherson, and R. L. Desjardins, Footprint prediction of scalar fluxes from analytical solutions of the diffusion equation, *Boundary Layer Meteorol.*, *50*, 355–373, 1990.

Smith, S. D., and E. P. Jones, Evidence for wind-pumping of air-sea gas exchange based on direct measurements of CO_2 fluxes, *J. Geophys. Res.*, *90*, 869–875, 1985.

Smith, S. D., and E. P. Jones, Isotopic and micrometeorological ocean CO_2 fluxes: Different time and space scales, *J. Geophys. Res.*, *91*, 10,529–10,532, 1986.

Smith, S. D., R. J. Anderson, E. P. Jones, R. L. Desjardins, R. M. Moore, O. Hertzman, and B. D. Johnson, A new measurement of CO_2 eddy flux in the nearshore atmospheric surface layer, *J. Geophys. Res.*, *96*, 8881–8887, 1991.

Soloviev, A. V., and P. Schluessel, Parameterization of the temperature difference across the cool skin of the ocean and of the air-ocean gas transfer on the basis of modelling surface renewal, *J. Phys. Oceanogr.*, *24*, 1319–1332, 1994.

Soloviev, A. V., and P. Schluessel, A model of air-sea gas exchange incorporating the physics of the turbulent boundary layer and the properties of the sea surface, in *Gas Transfer at Water Surfaces*, *Geophys. Monogr. Ser.*, vol. 127, edited by M. A. Donelan et al., pp. 141–146, AGU, Washington, D.C., 2001.

Soloviev, A. V., J. Edson, W. McGillis, P. Schluessel, and R. Wanninkof, Fine thermohaline structure and gas-exchange in the near-surface layer of the ocean during GasEx-98, in *Gas Transfer at Water Surfaces*, *Geophys. Monogr. Ser.*, vol. 127, edited by M. A. Donelan et al., pp. 181–185, AGU, Washington, D.C., 2001.

Stephens, D. W., Preliminary evaluation of the floating dome method for measuring reaeration rates, *J. Res. U.S. Geol. Surv.*, *6*, 547–552, 1978.

Stull, R. B., *An Introduction to Boundary Layer Meteorology*, 666 pp., Kluwer Acad., Norwell, Mass., 1988.

Sun, J., R. Desjardins, L. Marth, and I. MacPherson, Transport of carbon dioxide, water vapor, and ozone by turbulence and local circulations, *J. Geophys. Res.*, *103*, 25,873–25,885, 1998.

Sun, J., D. Vandemark, L. Mahrt, D. Vickers, T. Crawford, and C. Vogel, Momentum transfer over the coastal zone, *J. Geophys. Res.*, *106*, 12,437–12,448, 2001.

Suyker, A. E., and S. B. Verma, Eddy correlation measurements of CO_2 flux using a closed-path sensor: Theory and field tests against an open-path sensor, *Boundary Layer Meteorol.*, *64*, 391–407, 1996.

Wanninkhof, R., and W. M. McGillis, A cubic relationship between gas transfer and wind speed, *Geophys. Res. Lett.*, *26*, 1889–1893, 1999.

Webb, E. K., G. I. Pearman, and R. Leuning, Correction of flux measurements for density effects due to heat and water vapour transfer, *Q. J. R. Meteorol. Soc.*, *106*, 85–100, 1980.

Wesely, M. L., D. R. Cook, R. L. Hart, and R. M. Williams, Air-sea exchange of CO_2 and evidence for enhanced upwelling fluxes, *J. Geophys. Res.*, *87*, 8827–8832, 1982.

Whiteman, C. D., K. J. Allwine, L. J. Fritschen, M. M. Orgill, and J. R. Simpson, Deep valley radiation and surface energy budget microclimates. Part I: Radiation, *J. Appl. Meteorol.*, *28*, 414–426, 1989.

Wilks, D. S., *Statistical Methods in the Atmospheric Sciences*, 467 pp., Academic, San Diego, Calif., 1995.

Zeman, O., and N. O. Jensen, Modification of turbulence characteristics in flow over hills, *Q. J. R. Meteorol. Soc.*, *113*, 55–80, 1987.

F. S. Chapin III, Institute of Arctic Biology, University of Alaska, Fairbanks, AK 99775, USA.

W. Eugster, Geographical Institute, University of Bern, Hallerstraße 12, CH-3012 Bern, Switzerland. (eugster@giub.unibe.ch)

T. Jonas and A. Wüest, Swiss Federal Institute for Environmental Science and Technology, Mail Box 611, CH-8600 Dübendorf, Switzerland.

G. Kling, Department of Ecology and Evolutionary Biology, University of Michigan, 830 North University Avenue, Ann Arbor, MI 48109-1048, USA.

S. MacIntyre, Marine Science Institute and Institute for Computational Earth System Science, University of California, 6838 Ellison Hall, Santa Barbara, CA 93106, USA.

J. P. McFadden, Department of Ecology, Evolution, and Behavior, University of Minnesota, St. Paul, MN 55108, USA.

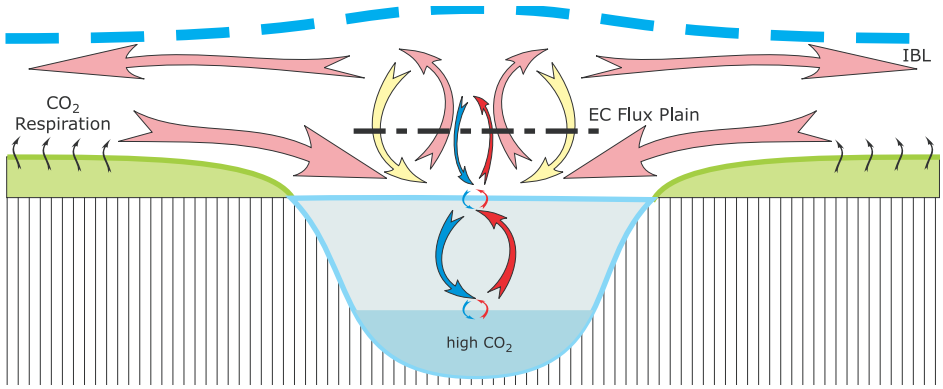

Figure 14. Processes influencing the eddy covariance (EC) flux measurements above a lake surface at night. Because EC measurements cannot be performed directly at the air-water interface, the CO_2 exchange with the lake (blue and red arrows) at EC reference height (black dash-dotted line) is measured together with the exchange flux of CO_2-rich air from the land surrounding the lake (pink and yellow arrows) where CO_2 originates from respiration of soils and vegetation (black arrows). This local lake-breeze type circulation is expected to be restricted in its vertical extent by an internal boundary layer (IBL).